

N72-31185

NASA TECHNICAL NOTE



NASA TN D-6959

NASA TN D-6959

CASE FILE  
COPY

NUMERICAL METHOD AND FORTRAN PROGRAM  
FOR THE SOLUTION OF AN AXISYMMETRIC  
ELECTROSTATIC COLLECTOR DESIGN PROBLEM

*by Oliver W. Reese*

*Lewis Research Center  
Cleveland, Ohio 44135*

NATIONAL AERONAUTICS AND SPACE ADMINISTRATION • WASHINGTON, D. C. • SEPTEMBER 1972

1. Report No. <b>NASA TN D-6959</b>		2. Government Accession No.		3. Recipient's Catalog No.	
4. Title and Subtitle <b>NUMERICAL METHOD AND FORTRAN PROGRAM FOR THE SOLUTION OF AN AXISYMMETRIC ELECTROSTATIC COLLECTOR DESIGN PROBLEM</b>				5. Report Date September 1972	
				6. Performing Organization Code	
7. Author(s) <b>Oliver W. Reese</b>				8. Performing Organization Report No. <b>E-6872</b>	
				10. Work Unit No. <b>111-05</b>	
9. Performing Organization Name and Address <b>Lewis Research Center National Aeronautics and Space Administration Cleveland, Ohio 44135</b>				11. Contract or Grant No.	
				13. Type of Report and Period Covered <b>Technical Note</b>	
12. Sponsoring Agency Name and Address <b>National Aeronautics and Space Administration Washington, D.C. 20546</b>				14. Sponsoring Agency Code	
15. Supplementary Notes					
16. Abstract <p>This report describes the numerical calculation of the steady-state flow of electrons in an axisymmetric, spherical, electrostatic collector for a range of boundary conditions. The trajectory equations of motion are solved alternately with Poisson's equation for the potential field until convergence is achieved. A direct (noniterative) numerical technique is used to obtain the solution to Poisson's equation. Space charge effects are included for initial current densities as large as <math>100 \text{ A/cm}^2</math>. Ways of dealing successfully with the difficulties associated with these high densities are discussed. The report includes a description of the mathematical model, a discussion of numerical techniques, results from two typical runs, and the FORTRAN computer program.</p>					
17. Key Words (Suggested by Author(s)) <b>FORTRAN                      Design</b> <b>Electrostatic                Poisson</b> <b>Collector</b>				18. Distribution Statement <b>Unclassified - unlimited</b>	
19. Security Classif. (of this report) <b>Unclassified</b>		20. Security Classif. (of this page) <b>Unclassified</b>		21. No. of Pages <b>67</b>	
				22. Price* <b>\$3.00</b>	

\* For sale by the National Technical Information Service, Springfield, Virginia 22151

# CONTENTS

	Page
SUMMARY . . . . .	1
INTRODUCTION . . . . .	1
STATEMENT OF THE PROBLEM . . . . .	4
METHOD OF SOLUTION . . . . .	5
Auxiliary Equations . . . . .	8
The Equation of Motion . . . . .	9
Poisson's Equation . . . . .	10
Calculation of Space Charge . . . . .	10
Use of Irregular Mesh Spacing . . . . .	13
Convergence Acceleration . . . . .	14
FORTRAN PROGRAM . . . . .	14
General Description . . . . .	14
Using the Program . . . . .	16
CONCLUDING REMARKS . . . . .	17
APPENDIXES	
A - SAMPLE PROBLEMS . . . . .	19
B - FORTRAN PROGRAM . . . . .	28
C - FORTRAN SYMBOLS . . . . .	50
D - FLOW CHARTS . . . . .	54
E - MAGNETIC FIELD CALCULATIONS . . . . .	57
F - DERIVATION OF EQUATIONS OF MOTION . . . . .	61
G - MATHEMATICAL SYMBOLS . . . . .	63
REFERENCES . . . . .	65

# NUMERICAL METHOD AND FORTRAN PROGRAM FOR THE SOLUTION OF AN AXISYMMETRIC ELECTROSTATIC COLLECTOR DESIGN PROBLEM

by Oliver W. Reese  
Lewis Research Center

## SUMMARY

This report describes the determination of the steady-state flow of electrons in an axisymmetric spherical collector under a variety of boundary conditions. The electron trajectory equations of motion are solved alternately with Poisson's equation for the potential field until convergence is achieved.

The bounding surfaces are a sphere below, a spherical cone above, and, optionally, a thin axial spike suspended from the apex of the cone. Negative decelerating potentials are prescribed on the cone-spike surface and on segmented zones of the spherical surface. Polar angles of the cone may vary from  $0^{\circ}$  to  $160^{\circ}$ .

The principal value of this report is that it pushes design research into the high-current-density range, where space charge effects are strong. Initial attempts met with convergence difficulties for current densities above  $50 \text{ A/cm}^2$ .

This report describes the method used to surmount these difficulties and handle values as high as  $100 \text{ A/cm}^2$ . This was achieved in two ways: first, by using variable mesh spacing to ensure accuracy in regions where the solution was changing rapidly; and second, by using a fast, accurate subprogram for obtaining the potential field. This subprogram uses a direct, noniterative numerical solution to Poisson's equation, the details of which are given in NASA TN D-6438.

The present report includes a description of the mathematical model, a discussion of numerical techniques, results from two typical runs, and the FORTRAN computer programs.

## INTRODUCTION

Satellite communication systems have been proposed in which the satellite can receive, amplify, and rebroadcast microwave signals. The high efficiency of the micro-

wave amplifiers to be used is of prime importance to the lifetime and reliability of such a system.

Microwave amplifiers, as a class, convert the energy of bunched electron beams into radiofrequency (rf) energy. Since this process is only partially efficient, the remaining beam energy is dissipated as heat in the electron collector. However, collectors can be designed and maintained at proper potentials to slow the electrons. The electron energy is then spent doing work against the collector potential and is recoverable as useful electrical power.

Reference 1 discusses how the results of the program described in this report are used in collector design. Reference 2 describes a computer program which solves Poisson's equation for a given space charge and which is required as a subroutine in the iterative solution of the current problem.

It is important to realize that there are two characteristics of electron beam trajectory patterns that facilitate efficient collector design:

- (1) Good, uniform, vertical and horizontal spreading (i. e. , a sufficient rise away from the entry hole, and a pushing away from the collector axis)
- (2) Good, uniform separation permitting insertion of electrodes to collect electrons near the peak of their trajectories, where their energy is close to minimum

Both these characteristics imply no backstreaming, crossing, or impingement of beams on the underside of the electrodes.

The original computer program dealt with negative decelerating potentials prescribed only on segmented zones of the sphere. But this approach was ineffective because of the great distance between these surface potentials and the incoming stream of electrons.

A second stage of the design was to prescribe a decelerating potential on a cone of varying polar angle. This slowed down the incoming stream considerably, and in most cases the beam spread was sufficient.

In other instances where even more beam spread was desirable, a third and final design modification was made. Here a negative potential was prescribed on a thin spike suspended from the cone. This had the effect of spreading the flow even more as it entered, and allowing the other decelerating potentials to come into play more effectively.

The final FORTRAN program reported herein allows for the presence or absence of an axial spike of varying length, as well as for the choice of decelerating surface potentials on zonal segments of the sphere and on the cone-spike surface. The cone angle varies from  $0^{\circ}$  to  $160^{\circ}$ . Initial conditions also include variable velocity and injection positions of entering electron groups.

It was assumed that, prior to entry into the collector, the electron beam had been sorted into graded velocity groups, with the outermost being the slowest. This is physically more realistic than assuming a constant velocity only. The beam was then

injected through a small entry hole in the collector where the negative polar axis pierces the spherical surface. The potential distribution on the surface of the sphere was assumed to be a function of the polar angle only. This report describes the numerical solution to a problem used in the design of such a collector under varying conditions of surface potential, current density, and collector geometry.

A typical configuration is shown in figure 1. Notice that the electron groups reach minimum velocity at their peaks and start falling back. If electrodes of the proper potential are inserted to collect the electrons at these minimum velocity points, the efficiency of the collector will then be maximized.

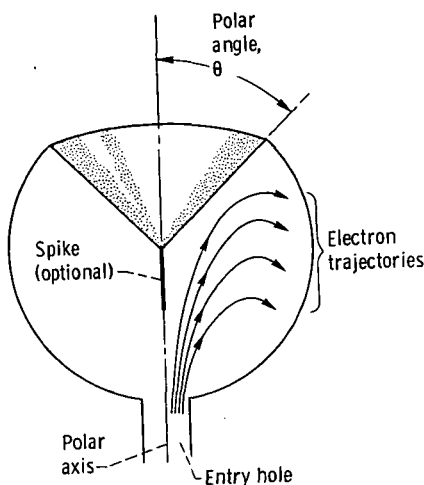


Figure 1. - Typical collector geometry (spherical cone).

The numerical technique and computer program described in reference 2 were used to determine the potential field inside the collector as required. The results were then used as part of the design criteria of the collector as described in reference 1.

In situations where current density is low, less than  $10 \text{ A/cm}^2$ , space charge effects were found to be negligible. But with higher current densities and associated higher space charge, certain problems arise near the entry hole that require special techniques to ensure numerical stability. This report describes these techniques. Current densities as high as  $100 \text{ A/cm}^2$  were dealt with successfully. Initially, calculations were successful only with current densities half as large, before numerical difficulties precluded further computation.

A complete description of the mathematical model is given, along with a discussion of the assumptions made. The technique used in determining the space charge distribution is then described. Appendixes A to G contain the results of two typical computer

runs, a complete listing of the FORTRAN computer program, flow charts, magnetic field calculations, the derivation of the equations of motion, and the mathematical symbols.

## STATEMENT OF THE PROBLEM

The problem is to determine the steady-state potential field and the associated steady-state electron beam trajectory patterns within a spherical collector (1) for any specified collector geometry (cone angle; collector radius; entry hole radius; and length of axial spike, if any), (2) for negative potential distribution on the surfaces of the collector, and (3) for magnetic field distribution and electron beam initial entry conditions (current, current density, perveance, injection angles, positioning, and velocity).

This involves the determination at every mesh point in the sphere of the potential  $V$  that satisfies Poisson's equation

$$\nabla^2 V = \bar{f}(V) \quad (1a)$$

where

$$\nabla^2 V = \frac{\partial^2 V}{\partial \bar{\rho}^2} + \frac{2}{\bar{\rho}} \frac{\partial V}{\partial \bar{\rho}} + \frac{1}{\bar{\rho}^2} \frac{\partial^2 V}{\partial \theta^2} + \frac{\cot \theta}{\bar{\rho}^2} \frac{\partial V}{\partial \theta} + \frac{1}{\bar{\rho}^2 \sin^2 \theta} \frac{\partial^2 V}{\partial \varphi^2} \quad (1b)$$

The bars refer to dimensioned values. All mathematical symbols are defined in appendix G. For convenience, these expressions and all others following are normalized by the substitution

$$\rho = \frac{\bar{\rho}}{R} \quad (1c)$$

We may now write

$$f(V) = \frac{\rho_e(V)}{\epsilon_0} \quad (1d)$$

The right-hand term in equation (1d) is related to space charge resulting from the beam trajectories. These trajectories are obtained from the solution to the differential equation of motion (eq. (3)). Note that the determination of  $V$  is an iterative process,

in that the right-hand side (or source term), which depends on the space charge, changes when the internal potential  $V$  changes.

The source term consists of the dielectric constant  $\epsilon_0$  and  $\rho_e(V)$  where

$$\rho_e(V) = \frac{|\vec{J}|}{|\vec{u}|} \quad (2)$$

The velocity term  $u$  is easily calculated since it is simply a function of certain initial conditions and the potentials  $V$  and  $V_m$ .

The current density term  $J$  is somewhat more complicated. In general, it is calculated from the current flow through annuli formed by adjacent trajectories of the various electron energy groups. This flow is shown later in figure 4. These trajectories are calculated from the differential equation of motion

$$\begin{aligned} \frac{\partial^2 \rho}{\partial \theta^2} = \rho'' = \rho + \frac{\rho \sin^2 \theta \dot{\varphi}^2}{\dot{\theta}^2} + \frac{\eta}{\dot{\theta}^2 R} \left( \frac{1}{R} \frac{\partial V}{\partial \rho} - \sin \theta \dot{\varphi} \frac{\partial V_m}{\partial \theta} \right) - \frac{\rho' \sin \theta \cos \theta \dot{\varphi}^2}{\dot{\theta}^2} \\ + \frac{2\rho'^2}{\rho} - \frac{\rho' \eta}{\rho^2 \dot{\theta}^2 R^2} \left( \frac{\partial V}{\partial \theta} + \rho^2 R \sin \theta \dot{\varphi} \frac{\partial V_m}{\partial \rho} \right) \end{aligned} \quad (3)$$

where

$\rho$  normalized radius vector

$\theta$  polar angle

$\varphi$  azimuthal angle

$R$  radius of sphere

$V_m$  magnetic field

Details of this iterative process are described in the next section.

## METHOD OF SOLUTION

First, the steady-state flow of electrons with a given velocity distribution was determined within the collector. This was accomplished by taking the following four steps:

(1) With the given collector geometry and a specified set of initial conditions, a first approximation to the potential field inside the collector was found by assuming zero space charge and solving Laplace's equation



$$\nabla^2 V = 0 \quad (4)$$

or

$$\frac{\partial^2 V}{\partial \rho^2} + \frac{2}{\rho} \frac{\partial V}{\partial \rho} + \frac{1}{\rho^2} \frac{\partial^2 V}{\partial \theta^2} + \frac{\cot \theta}{\rho^2} \frac{\partial V}{\partial \theta} = 0 \quad (5)$$

(2) An arbitrary number of equally spaced electron trajectories were then calculated from the equation of motion (eq. (3)). This equation is derived in appendix F. In general, nine electron groups were solved for in this problem.

(3) From these trajectory patterns, the space charge was then calculated at each mesh point, and the results were used as source terms in Poisson's equation which was solved next,

$$\nabla^2 V = \frac{\rho_e}{\epsilon_0} \quad (6)$$

Details of how the space charge was calculated are given in a later section.

(4) Equation (3) was solved again to obtain new trajectories based on the new potential field obtained from equation (6). This iterative process was then continued until convergence was achieved. The entire process is shown in flow chart form in figure 2.

Prior to solving the problem, the following four sets of normalized initial conditions must be specified. (The quantities listed in the first three sets are shown in figure 3 for the case of three electron classes.)

- (1) Collector geometry: radius of collector  $R$ , initial polar angle  $\theta_0$ , and radius of entry hole  $a$
- (2) Collector boundary values of electric potential: on a spherical surface ( $V_1, V_2, \dots, V_f$ ) (In general, the potential on the spherical surface decreases linearly to zero ( $V_f = 0$ ) as the polar angle increases from  $\theta_0$  to some prescribed  $\theta_f$ .); on a conical surface if  $\theta_0 \neq 0$  ( $V_1$ ); and along the negative polar axial spike if  $\theta_0 \neq 0$  ( $V_1$ ) (optional)
- (3) Electron beam entry conditions: type of flow (Brillouin or confined; confined flow means there is no initial rotational velocity of the beam, or  $\dot{\phi} = 0$ ), values of beam energy classes  $v_i$ , entry positions of electron classes in hole at injection  $\delta_i$  ( $\delta_i$  is the supplement of the polar angle  $\theta$ ), and entry angles  $\alpha_i$ . In general,  $i = 1, 2, \dots, 9$ .

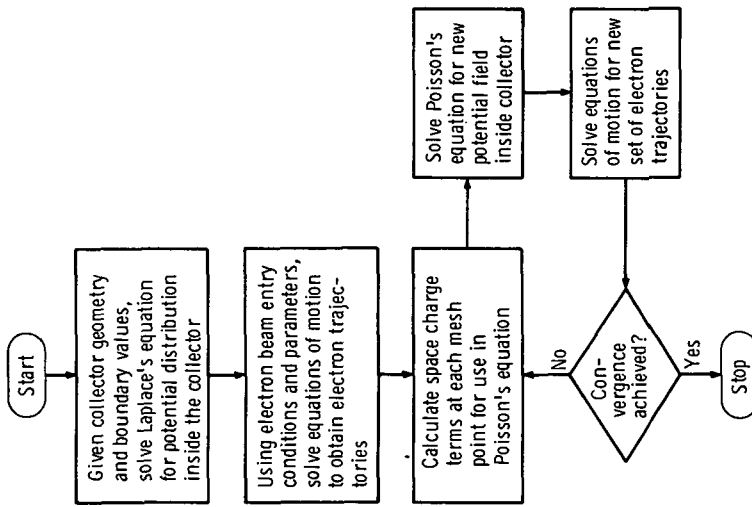


Figure 2. - Flow of operations in solution of complete problem.

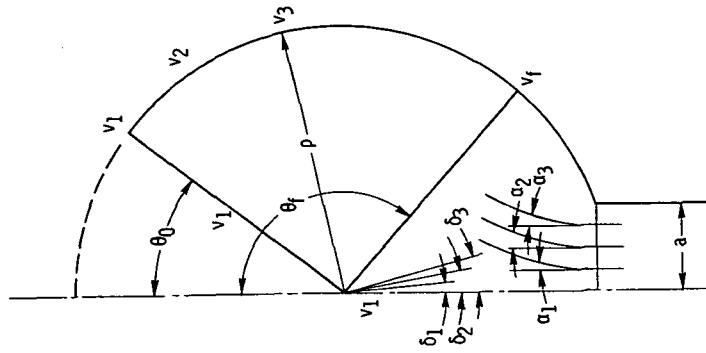


Figure 3. -  $\rho$ - $\theta$  plane of a typical axisymmetric collector, showing various initial conditions.

- (4) Electron beam parameters: magnetic flux density  $B_0$ , magnetic field potential  $V_m$ , electric potential  $V_0$ , current  $I_0$ , and current density  $J_0$

## Auxiliary Equations

We now discuss the auxiliary equations which are required in the solution of equation (3).

The first two are the magnetic field terms expressed in cylindrical coordinates.

$$\frac{\partial V_m}{\partial \rho} = R \left( \frac{\partial V_m}{\partial r} \sin \theta + \frac{\partial V_m}{\partial z} \cos \theta \right) \quad (7a)$$

$$\frac{\partial V_m}{\partial \theta} = \rho R \left( \frac{\partial V_m}{\partial r} \cos \theta - \frac{\partial V_m}{\partial z} \sin \theta \right) \quad (7b)$$

or letting  $B_r = \partial V_m / \partial r$  and  $B_z = \partial V_m / \partial z$ , then

$$\frac{\partial V_m}{\partial \rho} = R(B_r \sin \theta + B_z \cos \theta) \quad (8a)$$

$$\frac{\partial V_m}{\partial \theta} = \rho R(B_r \cos \theta - B_z \sin \theta) \quad (8b)$$

Prior to entering the collector, the electron beam passes through a magnetic field which is used to confine the beam. Part of this field leaks into the collector through the entry hole and influences the flow of the electrons. It must be considered in the equations of motion.

Also used are the velocity terms,  $\dot{\theta}^2$  and  $\dot{\phi}$ , and the magnetic flux  $\psi$ . These are expressed as

$$\dot{\theta}^2 = \frac{1}{1 + (\rho'/\rho)^2} \left[ \frac{2\eta_e V_0 (v_i + V)}{\rho^2 R^2} - \dot{\phi}^2 \sin^2 \theta \right] \quad (9)$$

$$\dot{\phi} = \frac{\eta_e (\psi - \psi_0)}{2\pi \rho^2 R^2 \sin^2 \theta} \quad (10)$$

$$\psi = 2\pi \int_0^r B_z r \, dr \quad (11)$$

which are equations (B16), (B8), and (B9) of reference 1, respectively.

Finally, the components  $B_r$  and  $B_z$  of the magnetic field  $V_m$  (eqs. (D9) and (D10) of ref. 1) are expressed as

$$B_r(r, z) = \sum_{n=0}^{\infty} \frac{(-1)^n}{n!(n+1)!} \times \frac{\partial^{2n+1} B(0, z)}{\partial z^{2n+1}} \times \left(\frac{r}{2}\right)^{2n+1} \quad (12)$$

and

$$B_z(r, z) = \sum_{n=1}^{\infty} \frac{(-1)^{n+1}}{[(n-1)!]^2} \times \frac{\partial^{2n-2} B(0, z)}{\partial z^{2n-2}} \times \left(\frac{r}{2}\right)^{2n-2} \quad (13)$$

where

$$B(0, z) = B_0 \left[ 1 - \frac{1}{\pi} \tan^{-1} \left( \frac{a}{-z} \right) - \frac{1}{\pi} \frac{z/a}{1 + (z^2/a^2)} \right] \quad (14)$$

The approximations of  $B_r(r, z)$  and  $B_z(r, z)$  that were used are given in appendix E.

## The Equation of Motion

The second-order differential equation of motion (eq. (3)) was transformed into two first-order equations and solved by using a fourth-order Runge-Kutta method. As is typical in integration techniques of this type, the choice of step size is based largely on experience. In this problem, the most critical region is near the entry hole. For a large collector radius ( $R = 16$  cm) and a small entry hole ( $a = 0.05$  cm), an initial step size  $\Delta\theta$  of  $0.01^\circ$  was required. For a small collector radius ( $R = 8$  cm) and a large entry hole ( $a = 0.10$  cm), an initial  $\Delta\theta$  of  $0.05^\circ$  was sufficient. As the trajectory moved away from this critical region, the  $\Delta\theta$  step was increased to minimize computer execution time.

Initially, the solution was obtained in the  $\rho$ - $\theta$  spherical plane. Then when any par-

ticular trajectory started to arc over ( $\rho' \cong 0$ ), a change was made to the  $r$ - $z$  cylindrical coordinate system to avoid any possible discontinuities in the integration process.

## Poisson's Equation

For any space charge field, the set of right-hand sides for Poisson's equation written at all interior grid points may be computed, and the subroutine of reference 2 may be applied to solve Poisson's equation for the internal potential field. The method of calculating the space charge field from the trajectory field is now presented.

## Calculation of Space Charge

The source term, or space charge term, in equation (6) is

$$\frac{\rho_e}{\epsilon_0} \quad (15)$$

where

$\epsilon_0$  dielectric constant,  $8.86 \times 10^{-14}$  F/cm (farads per centimeter)

$\rho_e$  volume charge density, C/cm<sup>3</sup> (coulombs per cubic centimeter)

Furthermore,

$$\rho_e = \frac{J}{u} \quad (16)$$

where

$J$  current density, A/cm<sup>2</sup> (amperes per square centimeter)

$u$  velocity, cm/sec

Figure 4 shows where a typical  $\rho_e$  is computed; namely, at a point midway between two trajectories. To ensure accuracy, space charge is calculated at selected points along center lines midway between adjacent trajectories where the  $\rho$ -mesh lines are crossed.

Since  $u$  is known at various points along a trajectory, one may interpolate to compute  $u$  at any point, say at a position midway between two trajectories. Therefore, the

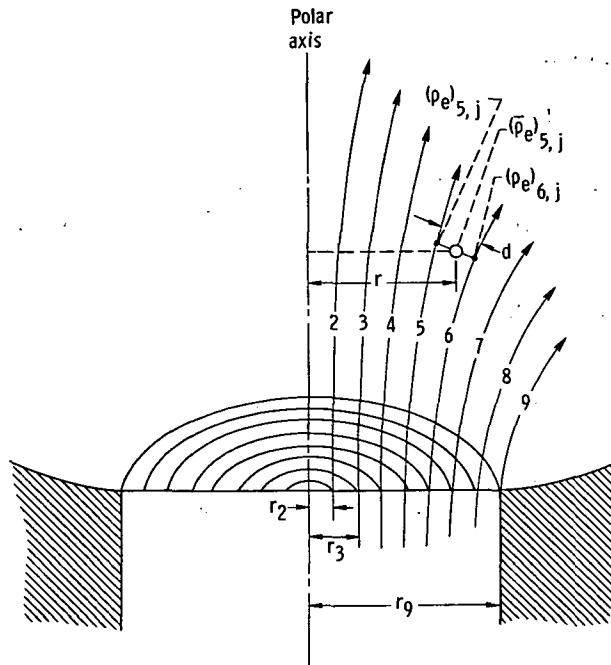


Figure 4. - Cross-sectional view of entry hole in spherical collector, showing typical injection pattern of electron energy groups 2 to 9 at radii  $r_2$ ,  $r_3$ , . . .  $r_9$ . First subscript refers to electron trajectory number; second subscript  $j$  refers to  $\rho$ -mesh line crossed by trajectory.

space charge at each mesh point may be determined once  $J$  is known. We now show how this is accomplished.

In general,

$$J = \frac{I}{A} \quad (17a)$$

where

$I$  current, A

$A$  any particular element of area through which current flows

Referring again to equation (6), we may now write

$$J_i = \frac{I_{0,i}}{A_i} \quad (17b)$$

where

$I_0$  initial current at injection

$i$   $i^{\text{th}}$  electron energy group

Referring again to figure 4, it is seen that the equally spaced electron energy groups form eight annuli at the entrance hole. The areas  $dA$  of these annuli may be expressed

$$\left. \begin{aligned} dA_1 &= \pi r_2^2 \\ dA_2 &= \pi r_3^2 - dA_1 = \pi(2r_2)^2 - dA_1 = 3 dA_1 \\ dA_3 &= \pi r_4^2 - \pi r_3^2 = \pi(3r_2)^2 - \pi(2r_2)^2 = 5 dA_1 \\ &\vdots \\ dA_8 &= \pi r_9^2 - \pi r_8^2 = \pi(8r_2)^2 - \pi(7r_2)^2 = 15 dA_1 \end{aligned} \right\} \quad (18)$$

Since  $I = JA$ , the current at injection through each annulus may be expressed

$$\left. \begin{aligned} I_{0,1} &= J_0 dA_1 \\ I_{0,2} &= J_0 dA_2 = 3J_0 dA_1 \\ I_{0,3} &= J_0 dA_3 = 5J_0 dA_1 \\ &\vdots \\ I_{0,8} &= J_0 dA_8 = 15J_0 dA_1 \\ &\vdots \\ I_{0,i} &= (2i - 1)J_0 dA_1 \end{aligned} \right\} \quad (19)$$

In the example of figure 4, the point shown represents a typical space coordinate midway between two adjacent trajectories, in this case, trajectories 5 and 6. The normal distance between the trajectories at this point is  $d$ . The area of the annulus is then

$$A = 2\pi r d = 2\pi \bar{\rho}_{5,j} \sin \bar{\theta}_{5,j} d \quad (20)$$

The general expression for the current density,  $J = I/A$  (eq. (17a)), may now be written as

$$J_{i,j} = \frac{(2i - 1)J_0 dA_1}{2\pi(\bar{\rho}_{i,j} \sin \bar{\theta}_{i,j}) d_{i,j}} \quad (21a)$$

or

$$J_{i,j} = \frac{(2i - 1)r_2^2 J_0}{2d_{i,j}(\bar{\rho}_{i,j} \sin \bar{\theta}_{i,j})} \quad (21b)$$

Notice that current is preserved in each annular region, namely

$$I_{0,i} = (2i - 1)J_0 dA_1 = J_{i,j} A_{i,j} \quad (22)$$

Since  $A_{i,j}$  can be computed at  $(\bar{\rho}_{i,j}, \bar{\theta}_{i,j})$  by

$$A_{i,j} = 2\pi \bar{\rho}_{i,j} \sin \bar{\theta}_{i,j} d_{i,j} \quad (23)$$

where  $d_{i,j}$  is the normal thickness of an annulus at this point.

### Use of Irregular Mesh Spacing

The successful solution to this problem, especially those phases dealing with high current densities, was largely due to the use of irregular mesh spacing in both the  $\rho$  and  $\theta$  directions. From figure 5 it is clearly apparent that the region in which the solution varies most rapidly is immediately along and adjacent to the negative polar axis, where the entering electron beam is most dense and of greatest velocity. Consequently, a closely spaced mesh was used in this region. Conversely, a coarse spacing was used where the solution was varying very slowly and quite predictably.



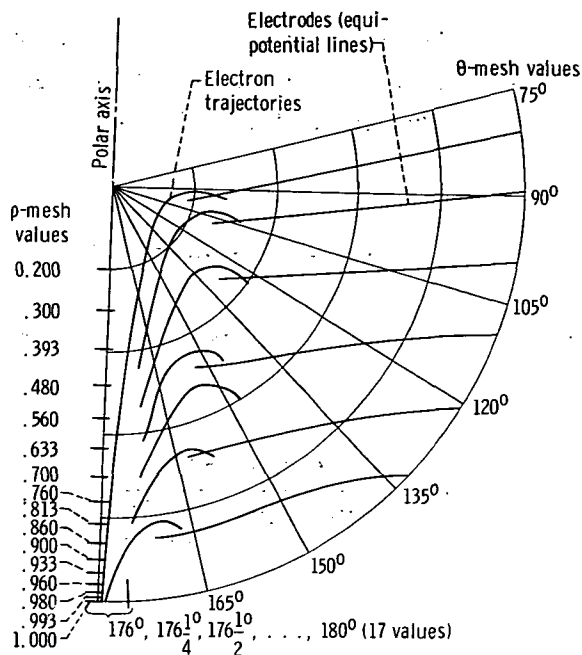


Figure 5. - Cross section of right half of spherical cone-shaped collector, showing typical pattern of electrodes, electron trajectories, and irregular mesh spacing in both the  $p$  and  $\theta$  directions.

## Convergence Acceleration

Experience has shown that in solving this problem, the iterants are well behaved and ultimately converge to an acceptable approximation to the solution. But because of the steadily decaying oscillatory nature of the iterants, a considerable savings in computer execution time was achieved by halving the newly calculated changes in the variables at each step. Normally, a maximum of five iterations would provide an acceptable solution.

## FORTRAN PROGRAM

### General Description

The program consists of the following 16 subroutines:

- (1) MAIN is the executive routine for processing multiple cases and has primary control of logical flow throughout the complete program.
- (2) INPUT reads and prints initial conditions, parameters, and other data required for internal use by the program (printout frequency, looping indices, convergence criteria, etc.).

(3) INTGRN controls integration looping of equations of motion, step size, change-over of coordinate systems, and the number of iterations required for convergence.

(4) DE is the spherical coordinate version of a routine for computing trajectories by integrating the equations of motion.

(5) DERIV calculates  $\partial V/\partial \rho$  and  $\partial V/\partial \theta$  for any specified interior point.

(6) RK is the spherical coordinate version of a Runge-Kutta integration subroutine used to compute trajectories.

(7) MESH generates graduated mesh point arrays in both the  $r$  and  $\theta$  directions for any specified collector geometry.

(8) RZTRAJ is the cylindrical coordinate version of a routine for computing trajectories by integrating equations of motion.

(9) RZRK is the cylindrical coordinate version of a Runge-Kutta integration subroutine used to compute trajectories.

(10) RZDE contains the equations of motion in the cylindrical coordinate system. It is similar to subroutine DE.

(11) OUT controls the printing of results at specified intervals along the trajectories.

(12) VFIELD provides for the calculation of the potential field for any particular set of boundary values and source terms. It uses the program described in reference 2.

(13) EQLINE calculates the spherical coordinates of any specified number of equipotential lines. It is used only after convergence is achieved in the main portion of the program.

(14) RHSCAL generates space charge values along center lines of the various annuli formed by the trajectories. It interpolates for these values at each mesh point, as required in the solution of Poisson's equation.

(15) PSICAL calculates the magnetic flux  $\psi$  of the magnetic field at each mesh point.

(16) BRBZ calculates  $B_r$  and  $B_z$ , the  $r$  and  $z$  components of the magnetic field, at each mesh point.

All calculations were done on the IBM 7094 II/7044 Direct Couple System computer. The program will perform about 210 integration steps per minute. This figure is based on trajectory calculations for eight electron energy groups.

About 15 000 storages are required for the program. This does not include that required for the solution of Poisson's equation. An additional 10 000 storage locations are needed for a solution to Poisson's equation similar to that described in reference 2.

The FORTRAN program is listed in appendix B, FORTRAN symbols are defined in appendix C, and flow charts are presented in appendix D.

## Using the Program

The program always starts by reading in a nine-card input data deck. The contents of each of these cards is now described.

### Card 1 (Format 55H. . .)

Contains any desired information to identify the particular case being run (card columns 1 to 55 only). This will be printed out at the top of a listing.

### Card 2 (Format 4E10.3)

R            radius of collector,  $R$ , cm  
B0           magnetic flux density,  $B_0$ , G  
DTHTD       $\theta$  step size used in Runge-Kutta integration (spherical coordinate),  
              $\Delta\theta$ , deg  
TH1         cone angle,  $\theta_1$ , deg

### Card 3 (Format 8E10.3)

ZI0           initial current<sup>1</sup>,  $I_0$ , A  
ZJ0           current density<sup>1</sup>,  $J_0$ , A/cm<sup>2</sup>  
V0            initial electric potential,  $V_0$ , V  
DELR         $r$  step size used in Runge-Kutta integration (cylindrical coordinates),  $\Delta r$   
CONFLO      indicates confined flow when equal to 1 and Brillouin flow when equal to 0  
RAD           radius of collector entry hole,  $a$ , cm  
FLOOP        number of iterations for space charge calculations (If no space charge calculation is desired, this value should be set to 1.)

### Card 4 (Format 40I2)

NT           number of trajectories to be calculated  
KPOI         printout frequency control, (e.g., 4 means to print results at every fourth integration step of a trajectory)  
  
N1 }  
N2 }           integrate trajectories N1 to N2 in steps of N3  
N3 }

---

<sup>1</sup>These two values are used only in the calculation of the source term in Poisson's equation when space charge iteration is necessary.

IBAR        when nonzero, indicates boundary values will be supplied along the  
             negative polar axis

LOOP        counter for number of space charge loops

KPOSC       print control for interim space charge calculations

Card 5 (Format 4F5.1)

These values are used by the integration subroutine in the spherical coordinate system, which is the system used in the beginning portion of the program.

THSFAC	}    step-size controls; increase step size DTH by a factor of THSFAC every THSDEL (deg) in the $\theta_5$ range from THSWHI (deg) to THSWLO (deg)
THSDEL	
THSWHI	
THSWLO	

Card 6 (Format 16F5.3)

VSMI(I),        electron energy classes for each of NT trajectories to be solved  
I = 1, NT        for

Card 7 (Format I2, 10F5.3)

This calculation is done only once, after convergence has been achieved in the main part of the program.

NEQL            number of equipotential lines to be calculated

EQL(I),        array of potential values for each equipotential line

I = 1, NEQL

Card 8 (Format 16F5.3)

XT(J, 16),       boundary values on surface of spherical collector from initial  
J = 1, 16        cone angle  $\theta_1$  to  $180^\circ$ , V

Card 9 (Format 16F5.3)

XT(J, 16)       continuation of card 8

J = 17, JF

Two sample test runs are given in appendix A. These runs were chosen to more clearly illustrate the makeup of the input data deck and to show the various options in output format available to the user.

## CONCLUDING REMARKS

We have described the numerical technique used to obtain a solution to a problem

associated with the design of an axisymmetric, spherical, depressed collector. Varying initial conditions include current density of electrons, surface potential on the collector, collector geometry, and the velocity and position of entering electron groups.

Of particular importance to the successful solution is the scheme used near the entry hole in the collector. Here the entering electron stream is of highest velocity and greatest density, giving rise to computational problems, especially in cases of high initial current densities.

Calculations by others in the past were successful in handling current densities to  $50 \text{ A/cm}^2$  before numerical difficulties precluded further computation. The numerical approach described in this report is used to solve systems with current densities to  $100 \text{ A/cm}^2$ .

Computational stability was achieved primarily by using a graduated mesh in both the  $r$  and  $\theta$  directions, with greatest mesh point density in the hole region. In addition, computational efficiency was improved by taking advantage of the fact that all entering electron groups were distributed uniformly both in positioning and velocity grouping. That is, the fastest group entered closest to the axis, and the slowest group entered nearest the edge of the entry hole.

Space charge effects were found to be negligible for initial current densities less than  $10 \text{ A/cm}^2$ . Consequently, the problem was reduced to requiring only one iteration and essentially solving Laplace's equation to obtain the potential distribution inside the collector.

Lewis Research Center,

National Aeronautics and Space Administration,

Cleveland, Ohio, June 2, 1972,

111-05.

## APPENDIX A

### SAMPLE PROBLEMS

Short, partial, representative computer output listings of two sample runs are presented. Run 1, depicted graphically in figure 6, is for a 0.2 spike, no space charge iterations, confined flow, and a cone angle of  $60^\circ$ . Run 2, figure 7, is for no spike, space charge effects calculated, Brillouin flow, and a cone angle of  $45^\circ$ .

Figure 7 shows a poor pattern. Beam spread and separation is rather nonuniform and erratic. In contrast, figure 6 shows well-shaped and well-behaved beams with good spread and uniform spacing.

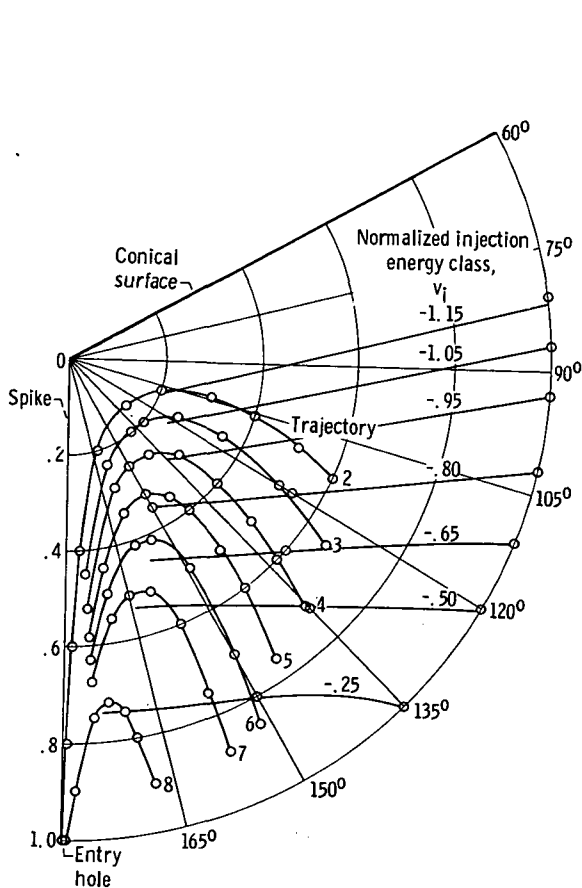


Figure 6. - Sample run 1. No iterations necessary (current density,  $8 \text{ A/cm}^2$ ); 0.2 spoke; cone angle,  $60^\circ$ .

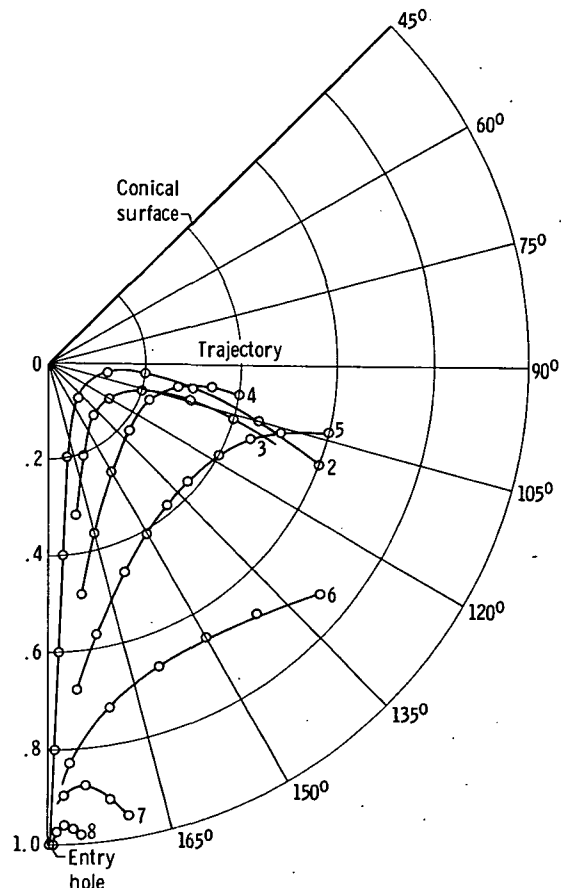


Figure 7. - Sample run 2. Five iterations for space charge effect; no spike; cone angle,  $60^\circ$ .

# Sample Run 1

SAMPLE RUN NO. 1

NO SPACE CHARGE EFFECTS  
CONFINED FLOW.

INPUT-

FO = 8.860E-14 KP = 6.158E-07  
CMFGA = 1.414E+10 ETAC = 1.753E+15  
IG = 4.000E-01  
JC = 2.050E+00 R = 8.000E+00  
VO = 7.500E+03 RO = 1.000E-06  
TAU02 = 0.243E-17 RAD = 0.400E+00

CUIPLT EVERY 4 STEPS.

INITIAL VALUES- I	DEL I (MAU)	DEL I (DEG)	THETA (DEG)	VSM	VI	INJEC. ANGLES	PSIO
2	0.106	0.358	179.642	0.900	6.75E+03	2.000	3.925E-09
3	0.013	0.716	179.284	0.800	6.00E+03	3.000	1.568E-08
4	0.019	1.074	178.926	0.700	5.25E+03	4.000	3.517E-08
5	0.025	1.433	178.567	0.600	4.50E+03	5.000	6.225E-08
6	0.031	1.791	178.209	0.500	3.75E+03	6.000	9.659E-08
7	0.038	2.149	177.851	0.400	3.00E+03	7.000	1.373E-07
8	0.044	2.507	177.493	0.200	1.50E+03	8.000	1.809E-07

EAR VALUES-

R  
0.000 -1.500  
0.200 -1.500  
0.300 -0.782  
0.393 -0.625  
0.480 -0.503  
0.560 -0.411  
0.633 -0.327  
0.700 -0.260  
0.760 -0.198  
0.813 -0.148  
0.860 -0.108  
0.900 -0.076  
0.933 -0.048  
0.960 -0.028  
0.980 -0.014  
0.993 -0.005  
1.000 0.

POTENTIAL FIELD

INPUT- THETA	0.560	0.633	0.700	0.760	0.813	0.860	0.900	0.933	0.960	0.980	0.993	1.000
60.00	-1.50E+00	-1.50E+00	-1.50E+00	-1.50E+00	-1.50E+00	-1.50E+00	-1.50E+00	-1.50E+00	-1.50E+00	-1.50E+00	-1.50E+00	-1.50E+00
75.00	0.	0.	0.	0.	0.	0.	0.	0.	0.	0.	0.	0.
90.00	0.	0.	0.	0.	0.	0.	0.	0.	0.	0.	0.	0.
105.00	0.	0.	0.	0.	0.	0.	0.	0.	0.	0.	0.	-1.25E+00
120.00	0.	0.	0.	0.	0.	0.	0.	0.	0.	0.	0.	-1.00E+00
135.00	0.	0.	0.	0.	0.	0.	0.	0.	0.	0.	0.	-7.50E-01
150.00	0.	0.	0.	0.	0.	0.	0.	0.	0.	0.	0.	-5.00E-01
165.00	0.	0.	0.	0.	0.	0.	0.	0.	0.	0.	0.	-2.50E-01
176.00	0.	0.	0.	0.	0.	0.	0.	0.	0.	0.	0.	0.
176.25	0.	0.	0.	0.	0.	0.	0.	0.	0.	0.	0.	0.
176.50	0.	0.	0.	0.	0.	0.	0.	0.	0.	0.	0.	0.
176.75	0.	0.	0.	0.	0.	0.	0.	0.	0.	0.	0.	0.
177.00	0.	0.	0.	0.	0.	0.	0.	0.	0.	0.	0.	0.
177.25	0.	0.	0.	0.	0.	0.	0.	0.	0.	0.	0.	0.
177.50	0.	0.	0.	0.	0.	0.	0.	0.	0.	0.	0.	0.
177.75	0.	0.	0.	0.	0.	0.	0.	0.	0.	0.	0.	0.
178.00	0.	0.	0.	0.	0.	0.	0.	0.	0.	0.	0.	0.
178.25	0.	0.	0.	0.	0.	0.	0.	0.	0.	0.	0.	0.
178.50	0.	0.	0.	0.	0.	0.	0.	0.	0.	0.	0.	0.
178.75	0.	0.	0.	0.	0.	0.	0.	0.	0.	0.	0.	0.
179.00	0.	0.	0.	0.	0.	0.	0.	0.	0.	0.	0.	0.
179.25	0.	0.	0.	0.	0.	0.	0.	0.	0.	0.	0.	0.
179.50	0.	0.	0.	0.	0.	0.	0.	0.	0.	0.	0.	0.
179.75	0.	0.	0.	0.	0.	0.	0.	0.	0.	0.	0.	0.
180.00	-4.11E-01	-3.27E-01	-2.60E-01	-1.98E-01	-1.48E-01	-1.08E-01	-7.57E-02	-4.80E-02	-2.80E-02	-1.40E-02	-4.60E-03	0.

x1=-1.50

POTENTIAL FIELD

OUTPUT- THETA	0.200	0.300	0.393	0.480	0.560	0.633	0.700	0.760	0.813	0.860	0.900	0.933	0.960	0.980	0.993	1.000
60.00	-1.5000	-1.5000	-1.5000	-1.5000	-1.5000	-1.5000	-1.5000	-1.5000	-1.5000	-1.5000	-1.5000	-1.5000	-1.5000	-1.5000	-1.5000	-1.5000
75.00	-1.3834	-1.3515	-1.3273	-1.3086	-1.2939	-1.2824	-1.2734	-1.2666	-1.2614	-1.2575	-1.2548	-1.2528	-1.2515	-1.2507	-1.2502	-1.2500
90.00	-1.2819	-1.2268	-1.1739	-1.1368	-1.1071	-1.0832	-1.0638	-1.0481	-1.0355	-1.0254	-1.0175	-1.0113	-1.0066	-1.0032	-1.0011	-1.0000
105.00	-1.1946	-1.1058	-1.0366	-0.9807	-0.9347	-0.8960	-0.8648	-0.8384	-0.8165	-0.7984	-0.7837	-0.7720	-0.7633	-0.7564	-0.7521	-0.7500
120.00	-1.1277	-1.0740	-1.0316	-0.9908	-0.9504	-0.9104	-0.8716	-0.8340	-0.7976	-0.7624	-0.7284	-0.6956	-0.6640	-0.6336	-0.6044	-0.5764
135.00	-1.0690	-1.0274	-0.9875	-0.9481	-0.9098	-0.8724	-0.8360	-0.7996	-0.7642	-0.7298	-0.6964	-0.6640	-0.6326	-0.6022	-0.5728	-0.5444
150.00	-1.0390	-0.9706	-0.9339	-0.8981	-0.8634	-0.8296	-0.7968	-0.7640	-0.7322	-0.7004	-0.6696	-0.6398	-0.6100	-0.5812	-0.5534	-0.5266
165.00	-1.0470	-0.9378	-0.8685	-0.8107	-0.7644	-0.7204	-0.6786	-0.6380	-0.5984	-0.5598	-0.5222	-0.4856	-0.4490	-0.4134	-0.3788	-0.3452
176.00	-1.1201	-0.9251	-0.8692	-0.8244	-0.7816	-0.7408	-0.7010	-0.6622	-0.6244	-0.5876	-0.5518	-0.5160	-0.4812	-0.4474	-0.4146	-0.3828
176.25	-1.1751	-0.9246	-0.8685	-0.8244	-0.7816	-0.7408	-0.7010	-0.6622	-0.6244	-0.5876	-0.5518	-0.5160	-0.4812	-0.4474	-0.4146	-0.3828
176.50	-1.1304	-0.9240	-0.8677	-0.8244	-0.7816	-0.7408	-0.7010	-0.6622	-0.6244	-0.5876	-0.5518	-0.5160	-0.4812	-0.4474	-0.4146	-0.3828
176.75	-1.1362	-0.9233	-0.8670	-0.8244	-0.7816	-0.7408	-0.7010	-0.6622	-0.6244	-0.5876	-0.5518	-0.5160	-0.4812	-0.4474	-0.4146	-0.3828
177.00	-1.1425	-0.9220	-0.8661	-0.8244	-0.7816	-0.7408	-0.7010	-0.6622	-0.6244	-0.5876	-0.5518	-0.5160	-0.4812	-0.4474	-0.4146	-0.3828
177.25	-1.1493	-0.9210	-0.8653	-0.8244	-0.7816	-0.7408	-0.7010	-0.6622	-0.6244	-0.5876	-0.5518	-0.5160	-0.4812	-0.4474	-0.4146	-0.3828
177.50	-1.1566	-0.9200	-0.8643	-0.8244	-0.7816	-0.7408	-0.7010	-0.6622	-0.6244	-0.5876	-0.5518	-0.5160	-0.4812	-0.4474	-0.4146	-0.3828
177.75	-1.1652	-0.9200	-0.8643	-0.8244	-0.7816	-0.7408	-0.7010	-0.6622	-0.6244	-0.5876	-0.5518	-0.5160	-0.4812	-0.4474	-0.4146	-0.3828
178.00	-1.1745	-0.9200	-0.8643	-0.8244	-0.7816	-0.7408	-0.7010	-0.6622	-0.6244	-0.5876	-0.5518	-0.5160	-0.4812	-0.4474	-0.4146	-0.3828
178.25	-1.1851	-0.9200	-0.8643	-0.8244	-0.7816	-0.7408	-0.7010	-0.6622	-0.6244	-0.5876	-0.5518	-0.5160	-0.4812	-0.4474	-0.4146	-0.3828
178.50	-1.1974	-0.9200	-0.8643	-0.8244	-0.7816	-0.7408	-0.7010	-0.6622	-0.6244	-0.5876	-0.5518	-0.5160	-0.4812	-0.4474	-0.4146	-0.3828

178.75-1.2120-0.8148-0.6577-0.5358-0.4361-0.3490-0.2754-0.2116-0.1583-0.1147-0.0794-0.0513-0.0300-0.0147-0.0048  
 179.00-1.2298-0.8128-0.6557-0.5338-0.4345-0.3476-0.2744-0.2108-0.1577-0.1142-0.0791-0.0511-0.0299-0.0147-0.0048  
 179.25-1.2578-0.8102-0.6530-0.5311-0.4324-0.3459-0.2731-0.2097-0.1568-0.1137-0.0788-0.0508-0.0297-0.0146-0.0048  
 179.50-1.2850-0.8075-0.6494-0.5274-0.4296-0.3434-0.2714-0.2082-0.1557-0.1129-0.0784-0.0504-0.0295-0.0145-0.0048  
 179.75-1.3337-0.8004-0.6433-0.5213-0.4249-0.3393-0.2685-0.2058-0.1537-0.1116-0.0777-0.0498-0.0291-0.0144-0.0047  
 180.00-1.5000-0.7820-0.6250-0.5213-0.4249-0.3393-0.2685-0.2058-0.1537-0.1116-0.0777-0.0498-0.0291-0.0144-0.0047

TABLE OF RHO-VALUES FOR  
EQUIPOTENTIAL LINES

THETA	-0.90	-0.80	-0.70	-0.60	-0.50	-0.40	-0.30	-0.20	-0.10
60.00	0.	0.	0.	0.	0.	0.	0.	0.	0.
75.00	0.	0.	0.	0.	0.	0.	0.	0.	0.
90.00	0.	0.	0.	0.	0.	0.	0.	0.	0.
105.00	0.627	0.856	0.	0.	0.	0.	0.	0.	0.
120.00	0.412	0.531	0.667	0.821	1.000	0.	0.	0.	0.
135.00	0.323	0.408	0.561	0.662	0.768	0.820	0.938	0.	0.
150.00	0.283	0.350	0.425	0.505	0.589	0.675	0.762	0.845	0.925
165.00	0.270	0.324	0.388	0.460	0.537	0.618	0.704	0.794	0.891
176.00	0.275	0.315	0.375	0.443	0.517	0.598	0.684	0.777	0.879
176.25	0.275	0.315	0.374	0.442	0.517	0.597	0.683	0.776	0.879
176.50	0.275	0.314	0.374	0.442	0.516	0.597	0.683	0.776	0.879
176.75	0.275	0.314	0.374	0.441	0.516	0.596	0.682	0.775	0.879
177.00	0.276	0.313	0.373	0.440	0.515	0.596	0.682	0.775	0.879
177.25	0.276	0.313	0.373	0.440	0.514	0.595	0.682	0.775	0.879
177.50	0.276	0.312	0.372	0.439	0.514	0.595	0.681	0.774	0.878
177.75	0.277	0.312	0.371	0.438	0.513	0.594	0.681	0.774	0.878
178.00	0.277	0.311	0.371	0.438	0.512	0.593	0.680	0.773	0.878
178.25	0.278	0.311	0.370	0.437	0.511	0.592	0.679	0.773	0.877
178.50	0.278	0.310	0.369	0.436	0.510	0.591	0.679	0.772	0.877
178.75	0.279	0.309	0.368	0.434	0.509	0.590	0.678	0.772	0.877
179.00	0.279	0.308	0.367	0.433	0.507	0.589	0.677	0.771	0.876
179.25	0.280	0.306	0.365	0.431	0.505	0.587	0.675	0.770	0.876
179.50	0.280	0.304	0.363	0.428	0.502	0.585	0.673	0.768	0.875
179.75	0.281	0.300	0.360	0.424	0.498	0.581	0.670	0.766	0.874
180.00	0.284	0.297	0.349	0.414	0.498	0.581	0.670	0.766	0.874

DNLTHETA=-0.0200 DEG.

TRJ	THETA	RHO	VT	DVDRH	DVDTH	RH-PR	RH-PPR	THDZ	PHDZ	PSI
STEP 0										
2	179.64	1.000	0.	0.	0.	2.408E+01	1.145E+03	6.366E+14	1.470E+12	3.914E-29
3	179.28	1.000	0.	0.	0.	1.531E+01	4.606E+02	1.396E+15	1.538E+12	1.563E-28
4	178.93	1.000	-0.	-0.	0.	1.122E+01	2.461E+02	2.267E+15	1.667E+12	3.577E-28
5	178.57	1.000	-0.	-0.	0.	8.842E+00	1.520E+02	3.113E+15	1.896E+12	6.256E-28
6	178.21	1.000	-0.	-0.	0.	7.290E+00	1.023E+02	3.794E+15	2.350E+12	9.625E-28
7	177.85	1.000	-0.	-0.	0.	6.196E+00	7.236E+01	4.172E+15	3.528E+12	1.367E-27
8	177.49	1.000	-0.	-0.	0.	5.382E+00	4.759E+01	2.743E+15	7.775E+12	1.797E-27
STEP 4										
2	179.56	0.967	-2.414E-02	5.592E+03	0.	2.317E+01	5.301E+02	6.694E+14	2.790E+16	1.830E-09
3	179.20	0.979	-1.554E-02	5.671E+03	0.	1.509E+01	-2.860E+01	1.409E+15	2.244E+16	9.319E-09
4	178.85	0.984	-1.147E-02	5.546E+03	0.	1.113E+01	-8.148E+01	2.267E+15	1.660E+16	2.355E-08
5	178.49	0.988	-0.097E-03	5.573E+03	0.	8.801E+00	-7.892E+01	3.095E+15	1.352E+16	4.413E-08
6	178.13	0.990	-7.539E-03	5.595E+03	0.	7.278E+00	-7.366E+01	3.750E+15	1.257E+16	6.974E-08
7	177.77	0.991	-4.441E-03	5.615E+03	0.	6.210E+00	-6.643E+01	4.089E+15	1.436E+16	9.643E-08
8	177.41	0.992	-5.646E-03	5.633E+03	0.	5.459E+00	-5.137E+01	2.593E+15	2.361E+16	1.102E-07
STEP 8										
2	179.48	0.935	-4.886E-02	5.857E+03	0.	2.209E+01	9.558E+02	7.155E+14	3.651E+16	7.893E-10
3	179.12	0.958	-3.160E-02	5.949E+03	0.	1.504E+01	1.546E+02	1.391E+15	4.761E+16	4.939E-09
4	178.77	0.969	-2.331E-02	5.724E+03	0.	1.124E+01	-4.931E+01	2.182E+15	4.321E+16	1.440E-08
5	178.41	0.975	-1.843E-02	5.754E+03	0.	8.936E+00	-8.828E+01	2.957E+15	3.827E+16	2.929E-08
6	178.05	0.980	-1.571E-02	5.779E+03	0.	7.400E+00	-8.199E+01	3.574E+15	3.552E+16	4.852E-08
7	177.69	0.983	-1.299E-02	5.615E+03	0.	6.295E+00	-5.047E+01	3.916E+15	3.486E+16	7.017E-08
8	177.33	0.985	-1.139E-02	5.637E+03	0.	5.457E+00	1.168E+01	2.518E+15	3.577E+16	8.977E-08
STEP 12										
2	179.40	0.906	-7.391E-02	6.253E+03	0.	2.065E+01	1.049E+03	7.943E+14	2.933E+16	4.148E-10
3	179.04	0.937	-4.816E-02	5.959E+03	0.	1.467E+01	3.465E+02	1.429E+15	5.111E+16	2.751E-09
4	178.69	0.953	-3.558E-02	5.951E+03	0.	1.122E+01	8.068E+01	2.152E+15	5.774E+16	8.831E-09
5	178.33	0.963	-2.808E-02	5.760E+03	0.	9.012E+00	-1.634E+01	2.860E+15	5.618E+16	1.933E-08
6	177.97	0.969	-2.324E-02	5.784E+03	0.	7.486E+00	-3.894E+01	3.436E+15	5.425E+16	3.358E-08
7	177.61	0.974	-1.977E-02	5.804E+03	0.	6.348E+00	-2.491E+01	3.786E+15	5.260E+16	5.061E-08
8	177.25	0.977	-1.770E-02	5.823E+03	0.	5.467E+00	-1.826E+01	2.432E+15	4.562E+16	7.342E-08
STEP 16										
2	179.37	0.878	-5.866E-02	6.515E+03	0.	1.921E+01	9.979E+02	8.907E+14	2.194E+16	2.587E-10
3	179.06	0.917	-4.500E-02	6.316E+03	0.	1.411E+01	4.349E+02	1.509E+15	4.920E+16	1.688E-09
4	178.71	0.937	-4.806E-02	5.958E+03	0.	1.104E+01	1.755E+02	2.182E+15	6.105E+16	5.676E-09
5	178.35	0.950	-3.811E-02	6.023E+03	0.	8.980E+00	5.802E+01	2.830E+15	6.438E+16	1.311E-08
6	177.99	0.959	-3.139E-02	6.044E+03	0.	7.506E+00	1.116E+01	3.361E+15	6.479E+16	2.379E-08
7	177.63	0.965	-2.666E-02	5.819E+03	0.	6.364E+00	2.516E+00	3.700E+15	6.474E+16	3.644E-08
8	177.27	0.969	-2.315E-02	5.827E+03	0.	5.485E+00	-3.021E+00	2.338E+15	6.183E+16	5.045E-08
STEP 20										
2	179.24	0.852	-1.212E-01	6.939E+03	0.	1.788E+01	9.212E+02	9.991E+14	1.650E+16	1.814E-10
3	178.88	0.898	-8.141E-02	6.597E+03	0.	1.349E+01	4.578E+02	1.615E+15	4.300E+16	1.132E-09

SWITCH TO R-Z COORDINATE SYSTEM-  
TRAJECTORY NO. 4 DEER=0.010

THETA	RHO	R	Z	DVDR	DVDZ	ZP	ZPP	V
167.39	0.388	0.085	-0.379	1.346E-01	-1.591E+00	1.836E-01	-2.520E+02	-6.967E-01
166.59	0.408	0.095	-0.397	1.097E-01	-1.388E+00	-3.808E+00	-2.384E+02	-6.684E-01
166.75	0.457	0.105	-0.445	1.153E-01	-1.387E+00	-5.494E+00	-1.190E+02	-6.014E-01
167.20	0.518	0.115	-0.505	9.988E-02	-1.284E+00	-6.469E+00	-7.624E+01	-5.207E-01
167.77	0.586	0.125	-0.573	9.760E-02	-1.218E+00	-7.083E+00	-5.065E+01	-4.342E-01
168.27	0.660	0.135	-0.646	1.015E-01	-1.162E+00	-7.488E+00	-3.238E+01	-3.458E-01
168.67	0.737	0.145	-0.722	1.113E-01	-1.111E+00	-7.729E+00	-1.723E+01	-2.580E-01
169.06	0.815	0.155	-0.800	1.166E-01	-1.014E+00	-7.844E+00	-5.895E+00	-1.730E-01
169.38	0.894	0.165	-0.879	1.359E-01	-9.620E-01	-7.840E+00	5.332E+00	-9.319E-02
169.65	0.973	0.175	-0.957	1.428E-01	-8.405E-01	-7.754E+00	1.205E+01	-2.276E-02
169.87	1.050	0.185	-1.034	1.627E-01	-8.097E-01	-7.607E+00	1.701E+01	4.139E-02



```

STEP 380
2 168.02 0.275 -8.922E-01 1.699E+04 -2.550E+02 -7.912E-02 1.201E+01 3.917E+16 2.703E+13 4.377E-11
3 167.66 0.325 -7.953E-01 1.188E+04 4.398E+02 1.515E-01 2.084E+01 1.513E+16 1.977E+14 7.952E-11
STEP 384
2 167.86 0.275 -8.915E-01 1.652E+04 -2.484E+02 -1.124E-01 1.183E+01 3.953E+16 2.554E+13 4.502E-11
3 167.50 0.325 -7.960E-01 1.187E+04 4.388E+02 1.517E-01 2.200E+01 1.456E+16 1.887E+14 8.117E-11
STEP 388
2 167.70 0.275 -8.906E-01 1.665E+04 -2.396E+02 -1.452E-01 1.170E+01 3.982E+16 2.411E+13 4.634E-11
3 167.34 0.325 -7.964E-01 1.186E+04 4.383E+02 2.838E-02 2.339E+01 1.395E+16 1.798E+14 8.299E-11

```

SWITCH TO R-Z COORDINATE SYSTEM-  
TRAJECTORY NO. 3 DELR=.010

THETA	RHO	R	Z	DVDR	DVDZ	ZP	ZPP	V
167.26	0.325	0.072	-0.317	1.733E-01	-1.582E+00	2.104E-01	-2.410E+02	-7.965E-01
166.18	0.342	0.082	-0.332	1.506E-01	-1.574E+00	-2.982E+00	-1.719E+02	-7.711E-01
166.03	0.380	0.092	-0.368	1.737E-01	-1.577E+00	-4.195E+00	-8.929E+01	-7.116E-01
166.22	0.427	0.102	-0.414	1.223E-01	-1.386E+00	-4.956E+00	-6.387E+01	-6.440E-01
166.55	0.480	0.112	-0.467	1.004E-01	-1.286E+00	-5.507E+00	-4.997E+01	-5.701E-01
166.94	0.538	0.122	-0.524	1.125E-01	-1.282E+00	-5.936E+00	-3.653E+01	-4.954E-01
167.32	0.600	0.132	-0.585	1.106E-01	-1.216E+00	-6.260E+00	-2.759E+01	-4.186E-01
167.69	0.664	0.142	-0.649	1.141E-01	-1.162E+00	-6.495E+00	-1.981E+01	-3.415E-01
168.02	0.731	0.152	-0.715	1.220E-01	-1.112E+00	-6.655E+00	-1.270E+01	-2.653E-01
168.32	0.799	0.162	-0.762	1.332E-01	-1.062E+00	-6.752E+00	-6.234E+00	-1.914E-01
168.58	0.867	0.172	-0.850	1.386E-01	-9.669E-01	-6.787E+00	-8.964E-01	-1.209E-01
168.80	0.935	0.182	-0.918	1.477E-01	-8.795E-01	-6.772E+00	3.810E+00	-5.565E-02
168.99	1.004	0.192	-0.985	1.601E-01	-8.159E-01	-6.715E+00	7.435E+00	3.030E-03

SWITCH TO R-Z COORDINATE SYSTEM-  
TRAJECTORY NO. 2 DELR=.010

THETA	RHO	R	Z	DVDR	DVDZ	ZP	ZPP	V
167.58	0.276	0.059	-0.269	5.909E-01	-2.163E+00	-3.479E-01	-1.075E+02	-8.898E-01
165.95	0.286	0.069	-0.277	5.171E-01	-2.083E+00	-1.088E+00	-5.181E+01	-8.680E-01
164.71	0.301	0.079	-0.290	8.156E-03	-1.617E+00	-1.529E+00	-4.258E+01	-8.371E-01
163.81	0.320	0.089	-0.308	1.875E-02	-1.611E+00	-1.949E+00	-4.147E+01	-8.089E-01
163.21	0.344	0.099	-0.329	2.085E-02	-1.608E+00	-2.359E+00	-4.063E+01	-7.740E-01
162.88	0.371	0.109	-0.355	1.629E-02	-1.609E+00	-2.764E+00	-4.034E+01	-7.326E-01
162.76	0.403	0.119	-0.384	-4.307E-02	-1.434E+00	-3.168E+00	-4.058E+01	-6.864E-01
162.82	0.438	0.129	-0.418	-3.963E-02	-1.433E+00	-3.579E+00	-4.157E+01	-6.385E-01
163.01	0.477	0.139	-0.456	-3.965E-02	-1.433E+00	-4.001E+00	-4.290E+01	-5.846E-01
163.32	0.520	0.149	-0.498	-6.120E-02	-1.340E+00	-4.442E+00	-4.495E+01	-5.283E-01
163.70	0.568	0.159	-0.545	-7.266E-02	-1.280E+00	-4.901E+00	-4.723E+01	-4.669E-01
164.15	0.620	0.169	-0.596	-6.173E-02	-1.275E+00	-5.378E+00	-4.828E+01	-4.019E-01
164.64	0.677	0.179	-0.653	-5.701E-02	-1.223E+00	-5.867E+00	-4.866E+01	-3.329E-01
165.14	0.738	0.189	-0.714	1.827E-01	-1.112E+00	-6.270E+00	1.057E+00	-2.610E-01
165.60	0.801	0.199	-0.776	1.873E-01	-1.065E+00	-6.252E+00	3.005E+00	-1.914E-01
165.99	0.864	0.209	-0.839	1.848E-01	-9.747E-01	-6.215E+00	4.456E+00	-1.256E-01
166.31	0.927	0.219	-0.901	1.954E-01	-9.267E-01	-6.158E+00	6.441E+00	-6.471E-02
166.59	0.989	0.229	-0.962	1.924E-01	-8.249E-01	-6.088E+00	7.400E+00	-9.440E-03
166.82	1.050	0.239	-1.022	2.100E-01	-8.192E-01	-6.007E+00	8.701E+00	4.229E-02

## Sample Run 2

SAMPLE RUN NO: 2  
5 ITERATIONS FOR SPACE  
CHARGE EFFECTS  
BRILLOUIN FLOW  
INPUT-  
EC = 8.860E-14 KP = 1.160E-07  
OMEGA = 1.414E+10 ETAO = 1.753E+15  
IC = 8.300E-02  
JO = 8.000E+01 P = 8.000E+00  
VO = 8.000E+03 RO = 1.000E-06  
TAUC2 = 0.228E-17 RAD = 0.100E+00

OUTPUT EVERY 6 STEPS.

INITIAL VALUES-	DELTA	THETA	VSM	VI	INJEC.	PSIG
I	(RAD)	(DEG)	(DEG)		ANGLES	
2	0.002	0.090	179.920	0.990	7.20E+03	2.000
3	0.003	0.179	179.821	0.880	6.40E+03	3.000
4	0.005	0.269	179.731	0.770	5.60E+03	4.000
5	0.006	0.358	179.642	0.660	4.80E+03	5.000
6	0.008	0.448	179.552	0.550	4.00E+03	6.000
7	0.009	0.537	179.463	0.440	3.20E+03	7.000
8	0.011	0.627	179.373	0.330	2.40E+03	8.000

\*\*\*NO PAO\*\*

PCTENTIAL FIELD

INPUT- THETA	0.560	0.673	0.760	0.760	0.813	0.860	0.900	0.933	0.960	0.980	0.993	1.000
45.00	-1.00E+00	-1.00E+00	-1.00E+00	-1.00E+00	-1.00E+00	-1.00E+00	-1.00E+00	-1.00E+00	-1.00E+00	-1.00E+00	-1.00E+00	-1.00E+00
60.00	0.00	0.00	0.00	0.00	0.00	0.00	0.00	0.00	0.00	0.00	0.00	0.00
75.00	0.00	0.00	0.00	0.00	0.00	0.00	0.00	0.00	0.00	0.00	0.00	0.00
90.00	0.00	0.00	0.00	0.00	0.00	0.00	0.00	0.00	0.00	0.00	0.00	0.00
105.00	0.00	0.00	0.00	0.00	0.00	0.00	0.00	0.00	0.00	0.00	0.00	0.00
120.00	0.00	0.00	0.00	0.00	0.00	0.00	0.00	0.00	0.00	0.00	0.00	0.00
135.00	0.00	0.00	0.00	0.00	0.00	0.00	0.00	0.00	0.00	0.00	0.00	0.00
150.00	0.00	0.00	0.00	0.00	0.00	0.00	0.00	0.00	0.00	0.00	0.00	0.00
165.00	0.00	0.00	0.00	0.00	0.00	0.00	0.00	0.00	0.00	0.00	0.00	0.00
175.25	0.00	0.00	0.00	0.00	0.00	0.00	0.00	0.00	0.00	0.00	0.00	0.00
176.50	0.00	0.00	0.00	0.00	0.00	0.00	0.00	0.00	0.00	0.00	0.00	0.00
176.75	0.00	0.00	0.00	0.00	0.00	0.00	0.00	0.00	0.00	0.00	0.00	0.00
177.00	0.00	0.00	0.00	0.00	0.00	0.00	0.00	0.00	0.00	0.00	0.00	0.00
177.25	0.00	0.00	0.00	0.00	0.00	0.00	0.00	0.00	0.00	0.00	0.00	0.00
177.50	0.00	0.00	0.00	0.00	0.00	0.00	0.00	0.00	0.00	0.00	0.00	0.00
177.75	0.00	0.00	0.00	0.00	0.00	0.00	0.00	0.00	0.00	0.00	0.00	0.00
178.00	0.00	0.00	0.00	0.00	0.00	0.00	0.00	0.00	0.00	0.00	0.00	0.00
178.25	0.00	0.00	0.00	0.00	0.00	0.00	0.00	0.00	0.00	0.00	0.00	0.00
178.50	0.00	0.00	0.00	0.00	0.00	0.00	0.00	0.00	0.00	0.00	0.00	0.00
178.75	0.00	0.00	0.00	0.00	0.00	0.00	0.00	0.00	0.00	0.00	0.00	0.00
179.00	0.00	0.00	0.00	0.00	0.00	0.00	0.00	0.00	0.00	0.00	0.00	0.00
179.25	0.00	0.00	0.00	0.00	0.00	0.00	0.00	0.00	0.00	0.00	0.00	0.00
179.50	0.00	0.00	0.00	0.00	0.00	0.00	0.00	0.00	0.00	0.00	0.00	0.00
179.75	0.00	0.00	0.00	0.00	0.00	0.00	0.00	0.00	0.00	0.00	0.00	0.00
180.00	0.00	0.00	0.00	0.00	0.00	0.00	0.00	0.00	0.00	0.00	0.00	0.00

X1=-1.00

POTENTIAL FIELD

OUTPUT- THETA	0.200	0.330	0.393	0.480	0.560	0.633	0.700	0.760	0.813	0.860	0.900	0.933	0.960	0.980	0.993	1.000
45.00	-1.00E+00	-1.00E+00	-1.00E+00	-1.00E+00	-1.00E+00	-1.00E+00	-1.00E+00	-1.00E+00	-1.00E+00	-1.00E+00	-1.00E+00	-1.00E+00	-1.00E+00	-1.00E+00	-1.00E+00	-1.00E+00
60.00	0.00	0.00	0.00	0.00	0.00	0.00	0.00	0.00	0.00	0.00	0.00	0.00	0.00	0.00	0.00	0.00
75.00	0.00	0.00	0.00	0.00	0.00	0.00	0.00	0.00	0.00	0.00	0.00	0.00	0.00	0.00	0.00	0.00
90.00	0.00	0.00	0.00	0.00	0.00	0.00	0.00	0.00	0.00	0.00	0.00	0.00	0.00	0.00	0.00	0.00
105.00	0.00	0.00	0.00	0.00	0.00	0.00	0.00	0.00	0.00	0.00	0.00	0.00	0.00	0.00	0.00	0.00
120.00	0.00	0.00	0.00	0.00	0.00	0.00	0.00	0.00	0.00	0.00	0.00	0.00	0.00	0.00	0.00	0.00
135.00	0.00	0.00	0.00	0.00	0.00	0.00	0.00	0.00	0.00	0.00	0.00	0.00	0.00	0.00	0.00	0.00
150.00	0.00	0.00	0.00	0.00	0.00	0.00	0.00	0.00	0.00	0.00	0.00	0.00	0.00	0.00	0.00	0.00
165.00	0.00	0.00	0.00	0.00	0.00	0.00	0.00	0.00	0.00	0.00	0.00	0.00	0.00	0.00	0.00	0.00
175.25	0.00	0.00	0.00	0.00	0.00	0.00	0.00	0.00	0.00	0.00	0.00	0.00	0.00	0.00	0.00	0.00
176.50	0.00	0.00	0.00	0.00	0.00	0.00	0.00	0.00	0.00	0.00	0.00	0.00	0.00	0.00	0.00	0.00
176.75	0.00	0.00	0.00	0.00	0.00	0.00	0.00	0.00	0.00	0.00	0.00	0.00	0.00	0.00	0.00	0.00
177.00	0.00	0.00	0.00	0.00	0.00	0.00	0.00	0.00	0.00	0.00	0.00	0.00	0.00	0.00	0.00	0.00
177.25	0.00	0.00	0.00	0.00	0.00	0.00	0.00	0.00	0.00	0.00	0.00	0.00	0.00	0.00	0.00	0.00
177.50	0.00	0.00	0.00	0.00	0.00	0.00	0.00	0.00	0.00	0.00	0.00	0.00	0.00	0.00	0.00	0.00
177.75	0.00	0.00	0.00	0.00	0.00	0.00	0.00	0.00	0.00	0.00	0.00	0.00	0.00	0.00	0.00	0.00
178.00	0.00	0.00	0.00	0.00	0.00	0.00	0.00	0.00	0.00	0.00	0.00	0.00	0.00	0.00	0.00	0.00
178.25	0.00	0.00	0.00	0.00	0.00	0.00	0.00	0.00	0.00	0.00	0.00	0.00	0.00	0.00	0.00	0.00
178.50	0.00	0.00	0.00	0.00	0.00	0.00	0.00	0.00	0.00	0.00	0.00	0.00	0.00	0.00	0.00	0.00
178.75	0.00	0.00	0.00	0.00	0.00	0.00	0.00	0.00	0.00	0.00	0.00	0.00	0.00	0.00	0.00	0.00
179.00	0.00	0.00	0.00	0.00	0.00	0.00	0.00	0.00	0.00	0.00	0.00	0.00	0.00	0.00	0.00	0.00
179.25	0.00	0.00	0.00	0.00	0.00	0.00	0.00	0.00	0.00	0.00	0.00	0.00	0.00	0.00	0.00	0.00
179.50	0.00	0.00	0.00	0.00	0.00	0.00	0.00	0.00	0.00	0.00	0.00	0.00	0.00	0.00	0.00	0.00
179.75	0.00	0.00	0.00	0.00	0.00	0.00	0.00	0.00	0.00	0.00	0.00	0.00	0.00	0.00	0.00	0.00
180.00	0.00	0.00	0.00	0.00	0.00	0.00	0.00	0.00	0.00	0.00	0.00	0.00	0.00	0.00	0.00	0.00

PASS 1 FOLLOWS-

DELTHETA=0.020 DEG.

TRJ	THETA	RHO	VT	DVDRH	DVOTH	RH-PR	RH-PPR	T-D2	PHD2	PSI
STEP	0									
2	179.91	1.000	0.00	0.00	0.00	2.715E+01	3.401E+03	5.244E+14	1.881E+17	2.428E-10
3	179.82	1.000	0.00	0.00	0.00	1.789E+01	1.881E+03	1.092E+15	1.878E+17	9.737E-10
4	179.73	1.000	0.00	0.00	0.00	1.334E+01	1.236E+03	1.715E+15	1.874E+17	2.182E-09
5	179.64	1.000	0.00	0.00	0.00	1.062E+01	9.154E+02	2.310E+15	1.867E+17	3.871E-09
6	179.55	1.000	0.00	0.00	0.00	8.921E+00	7.448E+02	2.786E+15	1.855E+17	6.025E-09
7	179.46	1.000	0.00	0.00	0.00	7.538E+00	6.558E+02	3.031E+15	1.831E+17	8.625E-09
8	179.37	1.000	0.00	0.00	0.00	6.576E+00	5.852E+02	1.981E+15	1.770E+17	1.154E-08
STEP	4									
5	179.27	0.979	-5.829E-03	2.257E+03	0.00	9.917E+00	2.274E+02	2.622E+15	5.154E+14	3.473E-10
STEP	12									
5	179.40	0.959	-1.259E-02	2.363E+03	0.00	9.460E+00	2.105E+02	2.852E+15	1.747E+12	9.959E-11
STEP	18									
5	179.28	0.939	-1.730E-02	2.364E+03	0.00	9.035E+00	1.958E+02	3.095E+15	2.064E+12	4.564E-11
STEP	26									
5	179.16	0.920	-2.299E-02	2.507E+03	0.00	8.638E+00	1.835E+02	3.351E+15	4.482E+11	2.784E-11
STEP	33									
5	179.04	0.903	-2.854E-02	2.507E+03	0.00	8.266E+00	1.713E+02	3.622E+15	1.385E+11	1.946E-11
STEP	36									
5	178.92	0.884	-3.418E-02	2.591E+03	0.00	7.917E+00	1.613E+02	3.907E+15	5.282E+10	1.478E-11
STEP	42									
5	178.80	0.873	-3.964E-02	2.651E+03	0.00	7.590E+00	1.509E+02	4.207E+15	2.452E+10	1.188E-11
STEP	48									
5	178.68	0.854	-4.504E-02	2.793E+03	0.00	7.283E+00	1.428E+02	4.522E+15	1.254E+10	9.922E-12
STEP	56									
5	178.56	0.839	-5.053E-02	2.923E+03	0.00	6.994E+00	1.339E+02	4.853E+15	1.037E+09	8.533E-12
STEP	64									
5	178.44	0.825	-5.578E-02	2.923E+03	0.00	6.722E+00	1.258E+02	5.200E+15	4.232E+09	7.504E-12
177.25	0.00	1.65E+01	2.222E+01	3.35E+01	4.55E+01	5.30E+01	4.47E+01	0.00	0.00	0.00
177.50	0.00	1.57E+01	2.10E+01	2.97E+01	4.34E+01	7.32E+01	1.05E+02	1.24E+02	0.00	0.00
177.75	0.00	1.48E+01	1.97E+01	2.79E+01	4.06E+0					

# PCTENTIAL FIELD

OUTPUT-  
THETA 0-200 0-300 0-393 0-480 0-560 0-633 0-700 0-760 0-813 0-860 0-900 0-933 0-960 0-980 0-993 1-000  
45.00-1.000-0.000-1.000-1.000-1.000-1.000-1.000-1.000-1.000-1.000-1.000-1.000-1.000-1.000-1.000  
60.00-0.885-0.863-0.841-0.819-0.793-0.764-0.731-0.694-0.653-0.608-0.560-0.508-0.453-0.395-0.333-0.267  
75.00-0.793-0.763-0.732-0.694-0.653-0.608-0.560-0.508-0.453-0.395-0.333-0.267-0.199-0.127-0.051-0.000  
90.00-0.734-0.697-0.659-0.618-0.574-0.527-0.477-0.424-0.367-0.305-0.238-0.166-0.091-0.014-0.000-0.000  
105.00-0.696-0.659-0.618-0.574-0.527-0.477-0.424-0.367-0.305-0.238-0.166-0.091-0.014-0.000-0.000  
120.00-0.675-0.638-0.597-0.554-0.508-0.458-0.404-0.346-0.283-0.215-0.147-0.070-0.000-0.000-0.000-0.000  
135.00-0.658-0.621-0.580-0.537-0.491-0.441-0.387-0.328-0.264-0.195-0.127-0.060-0.000-0.000-0.000-0.000  
150.00-0.631-0.594-0.553-0.509-0.462-0.412-0.358-0.299-0.235-0.166-0.097-0.030-0.000-0.000-0.000-0.000  
165.00-0.605-0.568-0.527-0.483-0.436-0.386-0.332-0.273-0.209-0.140-0.071-0.000-0.000-0.000-0.000-0.000  
180.00-0.580-0.543-0.502-0.458-0.411-0.361-0.307-0.248-0.184-0.115-0.046-0.000-0.000-0.000-0.000-0.000  
195.00-0.556-0.519-0.478-0.434-0.387-0.337-0.283-0.224-0.160-0.091-0.022-0.000-0.000-0.000-0.000-0.000  
210.00-0.533-0.496-0.455-0.411-0.364-0.314-0.260-0.201-0.137-0.068-0.000-0.000-0.000-0.000-0.000-0.000  
225.00-0.511-0.474-0.433-0.389-0.342-0.292-0.238-0.179-0.115-0.046-0.000-0.000-0.000-0.000-0.000-0.000  
240.00-0.490-0.453-0.412-0.368-0.321-0.271-0.217-0.158-0.094-0.025-0.000-0.000-0.000-0.000-0.000-0.000  
255.00-0.470-0.433-0.392-0.348-0.301-0.251-0.197-0.138-0.074-0.005-0.000-0.000-0.000-0.000-0.000-0.000  
270.00-0.450-0.413-0.372-0.328-0.281-0.231-0.177-0.118-0.054-0.000-0.000-0.000-0.000-0.000-0.000-0.000  
285.00-0.430-0.393-0.352-0.308-0.261-0.211-0.157-0.098-0.034-0.000-0.000-0.000-0.000-0.000-0.000-0.000  
300.00-0.410-0.373-0.332-0.288-0.241-0.191-0.137-0.078-0.014-0.000-0.000-0.000-0.000-0.000-0.000-0.000  
315.00-0.390-0.353-0.312-0.268-0.221-0.171-0.117-0.058-0.000-0.000-0.000-0.000-0.000-0.000-0.000-0.000  
330.00-0.370-0.333-0.292-0.248-0.201-0.151-0.097-0.038-0.000-0.000-0.000-0.000-0.000-0.000-0.000-0.000  
345.00-0.350-0.313-0.272-0.228-0.181-0.131-0.077-0.018-0.000-0.000-0.000-0.000-0.000-0.000-0.000-0.000  
360.00-0.330-0.293-0.252-0.208-0.161-0.111-0.057-0.000-0.000-0.000-0.000-0.000-0.000-0.000-0.000-0.000  
375.00-0.310-0.273-0.232-0.188-0.141-0.091-0.037-0.000-0.000-0.000-0.000-0.000-0.000-0.000-0.000-0.000  
390.00-0.290-0.253-0.212-0.168-0.121-0.071-0.017-0.000-0.000-0.000-0.000-0.000-0.000-0.000-0.000-0.000  
405.00-0.270-0.233-0.192-0.148-0.101-0.051-0.000-0.000-0.000-0.000-0.000-0.000-0.000-0.000-0.000-0.000  
420.00-0.250-0.213-0.172-0.128-0.081-0.031-0.000-0.000-0.000-0.000-0.000-0.000-0.000-0.000-0.000-0.000  
435.00-0.230-0.193-0.152-0.108-0.061-0.011-0.000-0.000-0.000-0.000-0.000-0.000-0.000-0.000-0.000-0.000  
450.00-0.210-0.173-0.132-0.088-0.041-0.000-0.000-0.000-0.000-0.000-0.000-0.000-0.000-0.000-0.000-0.000  
465.00-0.190-0.153-0.112-0.068-0.021-0.000-0.000-0.000-0.000-0.000-0.000-0.000-0.000-0.000-0.000-0.000  
480.00-0.170-0.133-0.092-0.048-0.001-0.000-0.000-0.000-0.000-0.000-0.000-0.000-0.000-0.000-0.000-0.000  
495.00-0.150-0.113-0.072-0.028-0.000-0.000-0.000-0.000-0.000-0.000-0.000-0.000-0.000-0.000-0.000-0.000  
510.00-0.130-0.093-0.052-0.008-0.000-0.000-0.000-0.000-0.000-0.000-0.000-0.000-0.000-0.000-0.000-0.000  
525.00-0.110-0.073-0.032-0.000-0.000-0.000-0.000-0.000-0.000-0.000-0.000-0.000-0.000-0.000-0.000-0.000  
540.00-0.090-0.053-0.012-0.000-0.000-0.000-0.000-0.000-0.000-0.000-0.000-0.000-0.000-0.000-0.000-0.000  
555.00-0.070-0.033-0.000-0.000-0.000-0.000-0.000-0.000-0.000-0.000-0.000-0.000-0.000-0.000-0.000-0.000  
570.00-0.050-0.013-0.000-0.000-0.000-0.000-0.000-0.000-0.000-0.000-0.000-0.000-0.000-0.000-0.000-0.000  
585.00-0.030-0.000-0.000-0.000-0.000-0.000-0.000-0.000-0.000-0.000-0.000-0.000-0.000-0.000-0.000-0.000  
600.00-0.010-0.000-0.000-0.000-0.000-0.000-0.000-0.000-0.000-0.000-0.000-0.000-0.000-0.000-0.000-0.000

PASS 4 FOLLOW-  
STEP 1  
5 179.64 1.000 -2.922E-02 3.510E+04 0. 1.062E+01 1.387E+03 2.201E+15 1.867E+17 3.871E-09  
STEP 2  
5 179.52 0.979 -1.270E-01 2.013E+04 0. 9.139E+00 3.983E+02 2.454E+15 6.183E+14 3.810E-10  
STEP 3  
5 179.40 0.951 -1.176E-01 2.081E+04 0. 8.347E+00 3.604E+02 2.655E+15 2.543E+13 1.164E-10  
STEP 4  
5 179.28 0.924 -1.098E-01 1.361E+04 0. 7.774E+00 2.593E+02 2.860E+15 3.436E+12 5.956E-11  
STEP 5  
5 179.16 0.899 -2.245E-01 1.199E+04 0. 7.264E+00 2.216E+02 3.069E+15 6.255E+11 3.845E-11  
STEP 6  
5 179.04 0.874 -2.456E-01 1.021E+04 0. 6.819E+00 2.041E+02 3.281E+15 2.771E+11 2.819E-11  
STEP 7  
5 178.92 0.850 -2.659E-01 1.285E+04 0. 6.408E+00 1.929E+02 3.494E+15 1.156E+11 2.736E-11  
STEP 8  
5 178.80 0.827 -2.859E-01 1.029E+04 0. 6.020E+00 1.782E+02 3.719E+15 5.617E+10 1.870E-11  
STEP 9  
5 178.68 0.805 -3.051E-01 1.313E+04 0. 5.660E+00 1.654E+02 3.941E+15 3.056E+10 1.624E-11  
STEP 10  
5 178.56 0.783 -3.234E-01 1.330E+04 0. 5.326E+00 1.540E+02 4.165E+15 1.812E+10 1.450E-11  
STEP 11  
5 178.44 0.762 -3.405E-01 1.036E+04 0. 5.042E+00 1.251E+02 4.391E+15 1.151E+10 1.322E-11  
STEP 12  
5 178.32 0.742 -3.509E-01 1.045E+04 0. 4.788E+00 1.073E+02 4.619E+15 7.659E+09 1.224E-11  
STEP 13  
5 178.20 0.722 -3.633E-01 1.054E+04 0. 4.550E+00 1.012E+02 4.848E+15 5.375E+09 1.147E-11  
STEP 14  
5 178.08 0.703 -3.752E-01 1.065E+04 0. 4.328E+00 1.037E+02 5.080E+15 3.891E+09 1.086E-11  
STEP 15  
5 177.96 0.684 -3.867E-01 1.076E+04 0. 4.135E+00 9.792E+01 5.312E+15 2.504E+09 1.037E-11  
STEP 16  
5 177.84 0.666 -3.981E-01 1.076E+03 0. 3.979E+00 9.838E+01 5.554E+15 2.222E+09 9.955E-12  
STEP 17  
5 177.72 0.647 -4.094E-01 1.076E+03 0. 3.960E+00 9.576E+01 5.755E+15 1.732E+09 9.557E-12  
STEP 18  
5 177.60 0.629 -4.205E-01 1.076E+03 0. 3.746E+00 9.332E+01 6.041E+15 1.374E+09 9.280E-12  
STEP 19  
5 177.48 0.612 -4.315E-01 1.076E+03 0. 3.637E+00 9.102E+01 6.293E+15 1.105E+09 8.999E-12  
STEP 20  
5 177.36 0.594 -4.424E-01 1.076E+03 0. 3.532E+00 8.888E+01 6.552E+15 9.144E+08 8.749E-12  
STEP 21  
5 177.24 0.577 -4.532E-01 1.076E+03 0. 3.432E+00 8.686E+01 6.816E+15 7.444E+08 8.527E-12  
STEP 22  
5 177.12 0.560 -4.639E-01 1.076E+03 0. 3.337E+00 8.484E+01 7.085E+15 6.211E+08 8.324E-12  
STEP 23  
5 177.00 0.543 -4.746E-01 1.076E+03 0. 3.243E+00 8.282E+01 7.323E+15 5.222E+08 8.136E-12  
STEP 24  
5 176.88 0.526 -4.853E-01 1.076E+03 0. 3.149E+00 8.080E+01 7.563E+15 4.431E+08 7.955E-12  
STEP 25  
5 176.76 0.509 -4.960E-01 1.076E+03 0. 3.055E+00 7.878E+01 7.804E+15 3.781E+08 7.781E-12  
STEP 26  
5 176.64 0.492 -5.067E-01 1.076E+03 0. 2.961E+00 7.676E+01 8.045E+15 3.245E+08 7.619E-12  
STEP 27  
5 176.52 0.475 -5.174E-01 1.076E+03 0. 2.867E+00 7.474E+01 8.286E+15 2.803E+08 7.454E-12  
STEP 28  
5 176.40 0.458 -5.281E-01 1.076E+03 0. 2.773E+00 7.272E+01 8.527E+15 2.432E+08 7.298E-12  
STEP 29  
5 176.28 0.441 -5.388E-01 1.076E+03 0. 2.679E+00 7.070E+01 8.768E+15 2.122E+08 7.150E-12  
STEP 30  
5 176.16 0.424 -5.495E-01 1.076E+03 0. 2.585E+00 6.868E+01 9.009E+15 1.867E+08 7.002E-12  
STEP 31  
5 176.04 0.407 -5.602E-01 1.076E+03 0. 2.491E+00 6.666E+01 9.250E+15 1.654E+08 6.851E-12  
STEP 32  
5 175.92 0.390 -5.709E-01 1.076E+03 0. 2.397E+00 6.464E+01 9.491E+15 1.441E+08 6.833E-12  
STEP 33  
5 175.80 0.373 -5.816E-01 1.076E+03 0. 2.303E+00 6.262E+01 9.732E+15 1.228E+08 6.774E-12  
STEP 34  
5 175.68 0.356 -5.923E-01 1.076E+03 0. 2.209E+00 6.060E+01 9.973E+15 1.015E+08 6.660E-12  
STEP 35  
5 175.56 0.339 -6.030E-01 1.076E+03 0. 2.115E+00 5.858E+01 1.0214E+16 8.007E+07

```

STEP 216
5 175.30 0.672 -2.259E+01 -1.715E+03 -4.398E+03 2.001E+00 3.502E+01 2.575E+16 5.349E+07 6.661E-12
STEP 222
5 175.20 0.669 -2.237E+01 -1.655E+03 -4.776E+03 1.991E+00 3.179E+01 2.770E+16 6.625E+07 6.646E-12
STEP 228
5 175.09 0.664 -2.216E+01 -1.594E+03 -4.657E+03 1.981E+00 2.903E+01 2.962E+16 6.609E+07 6.645E-12
STEP 234
5 174.96 0.660 -2.195E+01 -1.533E+03 -4.542E+03 1.950E+00 2.664E+01 3.156E+16 7.441E+07 6.640E-12
STEP 240
5 174.84 0.655 -2.178E+01 -1.472E+03 -4.431E+03 1.936E+00 2.461E+01 3.351E+16 6.547E+07 6.647E-12
STEP 246
5 174.73 0.652 -2.159E+01 -1.412E+03 -4.323E+03 1.755E+00 2.281E+01 3.547E+16 6.456E+07 6.653E-12
STEP 252
5 174.60 0.648 -2.142E+01 -1.351E+03 -4.218E+03 1.710E+00 2.123E+01 3.744E+16 6.385E+07 6.655E-12
STEP 258
5 174.48 0.645 -2.125E+01 -1.290E+03 -4.115E+03 1.657E+00 1.983E+01 3.943E+16 5.724E+07 6.675E-12
STEP 264
5 174.36 0.642 -2.109E+01 -1.230E+03 -4.015E+03 1.627E+00 1.859E+01 4.142E+16 5.256E+07 6.654E-12
STEP 270
5 174.24 0.638 -2.096E+01 -1.169E+03 -3.919E+03 1.599E+00 1.746E+01 4.343E+16 5.081E+07 6.702E-12
STEP 276
5 174.12 0.635 -2.079E+01 -1.108E+03 -3.822E+03 1.554E+00 1.646E+01 4.544E+16 4.808E+07 6.723E-12

```

PHS VALUES:

THI=179.642 THF = 174.251

AXIAL  
POTENTIAL  
DISTRIBUTION

RHO -V  
0.632 0.361  
0.766 0.397  
0.766 0.413  
0.873 0.395  
0.846 0.321  
0.900 0.269  
0.923 0.220  
0.960 0.177  
0.980 0.127  
0.992 0.067  
1.000 0.0

INITIAL VALUES-

I	DEL I (RAD)	DEL I (DEG)	THETA (DEG)	VSM	VI	INJEC. ANGLES	PSIO
2	0.002	0.090	179.910	0.933	7.20E+03	2.000	0.
3	0.003	0.179	179.821	0.893	6.40E+03	3.000	0.
4	0.005	0.269	179.731	0.793	5.60E+03	4.000	0.
5	0.006	0.358	179.642	0.693	4.80E+03	5.000	0.
6	0.009	0.448	179.552	0.593	4.00E+03	6.000	0.
7	0.009	0.537	179.463	0.493	3.20E+03	7.000	0.
8	0.011	0.627	179.373	0.393	2.40E+03	8.000	0.

\*\*\*END RAD\*\*\*

PCTENTIAL FIELD

INPUT- THETA	0.560	0.633	0.700	0.750	0.813	RHO 0.860	0.900	0.933	0.960	0.980	0.993	1.000
45.00 -1.00E+00	-1.00E+00	-1.00E+00	-1.00E+00	-1.00E+00	-1.00E+00	-1.00E+00	-1.00E+00	-1.00E+00	-1.00E+00	-1.00E+00	-1.00E+00	-1.00E+00
50.00 0.	0.	0.	0.	0.	0.	0.	0.	0.	0.	0.	0.	-8.00E-01
75.00 0.	0.	0.	0.	0.	0.	0.	0.	0.	0.	0.	0.	-6.00E-01
90.00 0.	0.	0.	0.	0.	0.	0.	0.	0.	0.	0.	0.	-4.00E-01
105.00 0.	0.	0.	0.	0.	0.	0.	0.	0.	0.	0.	0.	-2.00E-01
120.00 0.	0.	0.	0.	0.	0.	0.	0.	0.	0.	0.	0.	0.
135.00 0.	0.	0.	0.	0.	0.	0.	0.	0.	0.	0.	0.	0.
150.00 0.	0.	0.	0.	0.	0.	0.	0.	0.	0.	0.	0.	0.
165.00 0.	0.	0.	0.	0.	0.	0.	0.	0.	0.	0.	0.	0.
174.25 0.	2.04E+01	2.96E+01	4.49E+01	7.13E+01	2.44E+01	0.	0.	0.	0.	0.	0.	0.
176.50 0.	1.56E+01	2.72E+01	4.11E+01	5.81E+01	5.24E+01	0.	0.	0.	0.	0.	0.	0.
178.75 0.	1.08E+01	2.59E+01	3.85E+01	5.34E+01	1.03E+02	0.	0.	0.	0.	0.	0.	0.
177.00 0.	1.79E+01	2.45E+01	3.61E+01	5.68E+01	9.85E+01	0.	0.	0.	0.	0.	0.	0.
177.25 0.	1.71E+01	2.33E+01	3.39E+01	5.17E+01	7.53E+01	1.93E+02	0.	0.	0.	0.	0.	0.
177.50 0.	1.62E+01	2.20E+01	3.19E+01	4.92E+01	8.06E+01	1.48E+02	0.	0.	0.	0.	0.	0.
177.75 0.	1.51E+01	2.07E+01	2.99E+01	4.48E+01	7.26E+01	1.20E+02	0.	0.	0.	0.	0.	0.
178.00 0.	1.39E+01	1.92E+01	2.79E+01	4.16E+01	6.05E+01	1.04E+02	2.34E+02	0.	0.	0.	0.	0.
178.25 0.	1.27E+01	1.74E+01	2.59E+01	3.86E+01	4.12E+01	1.09E+02	2.07E+02	0.	0.	0.	0.	0.
178.50 0.	1.14E+01	1.59E+01	2.33E+01	3.54E+01	5.82E+01	9.94E+01	2.03E+02	0.	0.	0.	0.	0.
178.75 0.	0.89E+00	1.38E+01	2.05E+01	3.16E+01	5.10E+01	8.89E+01	1.76E+02	3.71E+02	0.	0.	0.	0.
179.00 0.	0.60E+00	1.16E+01	1.75E+01	2.71E+01	4.49E+01	7.94E+01	1.55E+02	3.44E+02	7.51E+02	0.	0.	0.
179.25 0.	0.45E+00	0.93E+00	1.34E+01	2.22E+01	3.73E+01	6.78E+01	1.34E+02	3.06E+02	7.02E+02	0.	0.	0.
179.50 0.	0.40E+00	0.99E+00	0.93E+00	1.55E+01	2.74E+01	5.16E+01	1.07E+02	2.35E+02	5.56E+02	1.29E+03	0.	0.
179.75 0.	0.29E+00	0.99E+00	0.69E+00	0.77E+00	1.40E+01	2.82E+01	6.35E+01	1.55E+02	3.92E+02	9.31E+02	0.	0.
180.00 0.	0.	0.	0.	0.	0.	0.	0.	0.	0.	0.	0.	0.

PCTENTIAL FIELD

OUTPUT- THETA	0.200	0.300	0.393	0.480	0.550	0.633	0.700	0.750	0.813	0.860	0.900	0.933	0.960	0.980	0.993	1.000
45.00 -1.0000-1.0000-1.0000-1.0000-1.0000-1.0000-1.0000-1.0000-1.0000-1.0000-1.0000-1.0000-1.0000-1.0000-1.0000-1.0000	-1.0000	-1.0000	-1.0000	-1.0000	-1.0000	-1.0000	-1.0000	-1.0000	-1.0000	-1.0000	-1.0000	-1.0000	-1.0000	-1.0000	-1.0000	-1.0000
50.00 -0.8954-0.8603-0.8421-0.8284-0.8182-0.8118-0.8055-0.8020-0.7999-0.7988-0.7984-0.7985-0.7989-0.7994-0.7998-0.8000	-0.8954	-0.8603	-0.8421	-0.8284	-0.8182	-0.8118	-0.8055	-0.8020	-0.7999	-0.7988	-0.7984	-0.7985	-0.7989	-0.7994	-0.7998	-0.8000
75.00 -0.7915-0.7456-0.7112-0.6845-0.6636-0.6472-0.6345-0.6248-0.6174-0.6118-0.6077-0.6046-0.6027-0.6013-0.6004-0.6000	-0.7915	-0.7456	-0.7112	-0.6845	-0.6636	-0.6472	-0.6345	-0.6248	-0.6174	-0.6118	-0.6077	-0.6046	-0.6027	-0.6013	-0.6004	-0.6000
90.00 -0.7140-0.6493-0.5999-0.5599-0.5271-0.4939-0.4774-0.4593-0.4437-0.4314-0.4216-0.4139-0.4082-0.4040-0.4013-0.4000	-0.7140	-0.6493	-0.5999	-0.5599	-0.5271	-0.4939	-0.4774	-0.4593	-0.4437	-0.4314	-0.4216	-0.4139	-0.4082	-0.4040	-0.4013	-0.4000
105.00 -0.6498-0.5804-0.5067-0.4543-0.4094-0.3733-0.3362-0.3065-0.2811-0.2596-0.2417-0.2273-0.2161-0.2075-0.2026-0.2000	-0.6498	-0.5804	-0.5067	-0.4543	-0.4094	-0.3733	-0.3362	-0.3065	-0.2811	-0.2596	-0.2417	-0.2273	-0.2161	-0.2075	-0.2026	-0.2000
120.00 -0.5984-0.5068-0.4342-0.3725-0.3192-0.2693-0.2247-0.1839-0.1465-0.1126-0.0824-0.0561-0.0343-0.0174-0.0059-0.0000	-0.5984	-0.5068	-0.4342	-0.3725	-0.3192	-0.2693	-0.2247	-0.1839	-0.1465	-0.1126	-0.0824	-0.0561	-0.0343	-0.0174	-0.0059	-0.0000
135.00 -0.5601-0.4624-0.3846-0.3202-0.2683-0.2251-0.1877-0.1538-0.1213-0.0939-0.0514-0.0334-0.0196-0.0096-0.0032-0.0000	-0.5601	-0.4624	-0.3846	-0.3202	-0.2683	-0.2251	-0.1877	-0.1538	-0.1213	-0.0939	-0.0514	-0.0334	-0.0196	-0.0096	-0.0032	-0.0000
150.00 -0.5338-0.4329-0.3575-0.2969-0.2459-0.2013-0.1615-0.1261-0.0954-0.0694-0.0481-0.0312-0.0183-0.0090-0.0029-0.0000	-0.5338	-0.4329	-0.3575	-0.2969	-0.2459	-0.2013	-0.1615	-0.1261	-0.0954	-0.0694	-0.0481	-0.0312	-0.0183	-0.0090	-0.0029	-0.0000
165.00 -0.5187-0.4191-0.3501-0.3018-0.2679-0.2413-0.2131-0.1813-0.1455-0.1093-0.0769-0.0503-0.0295-0.0145-0.0048-0.0000	-0.5187	-0.4191	-0.3501	-0.3018	-0.2679	-0.2413	-0.2131	-0.1813	-0.1455	-0.1093	-0.0769	-0.0503	-0.0295	-0.0145	-0.0048	-0.0000
174.25 -0.5142-0.4156-0.3517-0.3181-0.2811-0.2450-0.2119-0.1750-0.1447-0.1130-0.0825-0.0521-0.0220-0.0044-0.0018-0.0000	-0.5142	-0.4156	-0.3517	-0.3181	-0.2811	-0.2450	-0.2119	-0.1750	-0.1447	-0.1130	-0.0825	-0.0521	-0.0220	-0.0044	-0.0018	-0.0000
176.50 -0.5141-0.4156-0.3517-0.3181-0.2811-0.2450-0.2119-0.1750-0.1447-0.1130-0.0825-0.0521-0.0220-0.0044-0.0018-0.0000	-0.5141	-0.4156	-0.3517	-0.3181	-0.2811	-0.2450	-0.2119	-0.1750	-0.1447	-0.1130	-0.0825	-0.0521	-0.0220	-0.0044	-0.0018	-0.0000
178.75 -0.5241-0.4156-0.3517-0.3181-0.2811-0.2450-0.2119-0.1750-0.1447-0.1130-0.0825-0.0521-0.0220-0.0044-0.0018-0.0000	-0.5241	-0.4156	-0.3517	-0.3181	-0.2811	-0.2450	-0.2119	-0.1750	-0.1447	-0.1130	-0.0825	-0.0521	-0.0220	-0.0044	-0.0018	-0.0000
177.00 -0.5141-0.4156-0.3517-0.3181-0.2811-0.2450-0.2119-0.1750-0.1447-0.1130-0.0825-0.0521-0.0220-0.0044-0.0018-0.0000	-0.5141	-0.4156	-0.3517	-0.3181	-0.2811	-0.2450	-0.2119	-0.1750	-0.1447	-0.1130	-0.0825	-0.0521	-0.0220	-0.0044	-0.0018	-0.0000
177.25 -0.5141-0.4156-0.3517-0.3181-0.2811-0.2450-0.2119-0.1750-0.1447-0.1130-0.0825-0.0521-0.0220-0.0044-0.0018-0.0000	-0.5141	-0.4156	-0.3517	-0.3181	-0.2811	-0.2450	-0.2119	-0.1750	-0.1447	-0.1130	-0.0825	-0.0521	-0.0220	-0.0044	-0.0018	-0.0000



97.24	0.257	0.255	-0.033	5.795E-01	-1.168E+00	-2.837E-01	-2.098E+00	-6.416E-01
97.52	0.269	0.265	-0.035	5.784E-01	-1.153E+00	-3.041E-01	-1.994E+00	-6.224E-01
97.99	0.278	0.275	-0.033	5.772E-01	-1.140E+00	-3.236E-01	-1.900E+00	-6.230E-01
98.16	0.288	0.285	-0.042	5.760E-01	-1.128E+00	-3.422E-01	-1.814E+00	-6.125E-01
98.75	0.290	0.285	-0.045	5.746E-01	-1.117E+00	-3.599E-01	-1.736E+00	-6.028E-01
99.15	0.300	0.305	-0.049	4.505E-01	-1.086E+00	-3.773E-01	-1.717E+00	-5.951E-01
99.54	0.320	0.315	-0.053	4.492E-01	-1.075E+00	-3.942E-01	-1.655E+00	-5.864E-01
99.94	0.330	0.325	-0.057	4.478E-01	-1.065E+00	-4.114E-01	-1.597E+00	-5.776E-01
100.35	0.341	0.335	-0.061	4.465E-01	-1.056E+00	-4.261E-01	-1.544E+00	-5.687E-01
100.75	0.351	0.345	-0.056	4.451E-01	-1.048E+00	-4.413E-01	-1.494E+00	-5.597E-01
101.15	0.362	0.355	-0.070	4.438E-01	-1.043E+00	-4.560E-01	-1.447E+00	-5.506E-01
101.55	0.373	0.365	-0.075	4.425E-01	-1.032E+00	-4.703E-01	-1.404E+00	-5.412E-01
101.95	0.383	0.375	-0.079	4.412E-01	-1.026E+00	-4.841E-01	-1.362E+00	-5.320E-01
102.35	0.394	0.385	-0.084	4.400E-01	-1.020E+00	-4.976E-01	-1.322E+00	-5.226E-01
102.74	0.405	0.395	-0.089	4.387E-01	-1.014E+00	-5.110E-01	-1.282E+00	-5.135E-01
103.14	0.416	0.405	-0.095	4.374E-01	-1.008E+00	-5.241E-01	-1.241E+00	-5.045E-01
103.52	0.427	0.415	-0.100	4.361E-01	-1.002E+00	-5.368E-01	-1.201E+00	-4.954E-01
103.91	0.438	0.425	-0.105	4.348E-01	-1.000E+00	-5.493E-01	-1.161E+00	-4.876E-01
104.29	0.449	0.435	-0.111	4.335E-01	-1.000E+00	-5.615E-01	-1.120E+00	-4.798E-01
104.67	0.460	0.445	-0.117	4.322E-01	-1.000E+00	-5.734E-01	-1.081E+00	-4.720E-01
105.04	0.471	0.455	-0.122	4.309E-01	-1.000E+00	-5.846E-01	-1.042E+00	-4.642E-01
105.41	0.482	0.465	-0.128	4.296E-01	-1.000E+00	-5.959E-01	-1.003E+00	-4.564E-01
105.77	0.493	0.475	-0.134	4.283E-01	-1.000E+00	-6.071E-01	-9.64E-01	-4.486E-01
106.12	0.505	0.485	-0.140	4.270E-01	-1.000E+00	-6.183E-01	-9.22E-01	-4.408E-01
106.47	0.516	0.495	-0.146	4.257E-01	-1.000E+00	-6.295E-01	-8.80E-01	-4.330E-01
106.80	0.528	0.505	-0.153	4.244E-01	-1.000E+00	-6.407E-01	-8.38E-01	-4.252E-01
107.14	0.539	0.515	-0.159	4.231E-01	-1.000E+00	-6.519E-01	-7.96E-01	-4.174E-01
107.46	0.551	0.525	-0.165	4.218E-01	-1.000E+00	-6.631E-01	-7.54E-01	-4.096E-01
107.79	0.562	0.535	-0.172	4.205E-01	-1.000E+00	-6.743E-01	-7.12E-01	-4.018E-01
108.10	0.574	0.545	-0.178	4.192E-01	-1.000E+00	-6.855E-01	-6.70E-01	-3.940E-01
108.41	0.585	0.555	-0.185	4.179E-01	-1.000E+00	-6.967E-01	-6.28E-01	-3.862E-01
108.71	0.597	0.565	-0.191	4.166E-01	-1.000E+00	-7.079E-01	-5.86E-01	-3.784E-01
109.01	0.608	0.575	-0.198	4.153E-01	-1.000E+00	-7.191E-01	-5.44E-01	-3.706E-01
109.31	0.620	0.585	-0.205	4.140E-01	-1.000E+00	-7.303E-01	-5.02E-01	-3.628E-01
109.59	0.632	0.595	-0.212	4.127E-01	-1.000E+00	-7.415E-01	-4.60E-01	-3.550E-01
109.88	0.644	0.605	-0.219	4.114E-01	-1.000E+00	-7.527E-01	-4.18E-01	-3.472E-01
110.16	0.655	0.615	-0.226	4.101E-01	-1.000E+00	-7.639E-01	-3.76E-01	-3.394E-01
110.44	0.667	0.625	-0.233	4.088E-01	-1.000E+00	-7.751E-01	-3.34E-01	-3.316E-01
110.71	0.679	0.635	-0.240	4.075E-01	-1.000E+00	-7.863E-01	-2.92E-01	-3.238E-01
110.98	0.691	0.645	-0.247	4.062E-01	-1.000E+00	-7.975E-01	-2.50E-01	-3.160E-01
111.24	0.703	0.655	-0.255	4.049E-01	-1.000E+00	-8.087E-01	-2.08E-01	-3.082E-01
111.50	0.715	0.665	-0.262	4.036E-01	-1.000E+00	-8.199E-01	-1.66E-01	-3.004E-01
111.76	0.727	0.675	-0.269	4.023E-01	-1.000E+00	-8.311E-01	-1.24E-01	-2.926E-01
112.01	0.739	0.685	-0.277	4.010E-01	-1.000E+00	-8.423E-01	-8.2E-02	-2.848E-01
112.26	0.751	0.695	-0.285	4.000E-01	-1.000E+00	-8.535E-01	-3.8E-02	-2.770E-01
112.51	0.763	0.705	-0.292	3.987E-01	-1.000E+00	-8.647E-01	6.0E-03	-2.692E-01
112.75	0.775	0.715	-0.300	3.974E-01	-1.000E+00	-8.759E-01	0.00E+00	-2.614E-01
112.99	0.788	0.725	-0.308	3.961E-01	-1.000E+00	-8.871E-01	0.00E+00	-2.536E-01
113.23	0.800	0.735	-0.315	3.948E-01	-1.000E+00	-8.983E-01	0.00E+00	-2.458E-01
113.46	0.812	0.745	-0.323	3.935E-01	-1.000E+00	-9.095E-01	0.00E+00	-2.380E-01
113.69	0.825	0.755	-0.331	3.922E-01	-1.000E+00	-9.207E-01	0.00E+00	-2.302E-01
113.92	0.837	0.765	-0.339	3.909E-01	-1.000E+00	-9.319E-01	0.00E+00	-2.224E-01
114.15	0.850	0.775	-0.348	3.896E-01	-1.000E+00	-9.431E-01	0.00E+00	-2.146E-01
114.37	0.862	0.785	-0.356	3.883E-01	-1.000E+00	-9.543E-01	0.00E+00	-2.068E-01
114.60	0.875	0.795	-0.364	3.870E-01	-1.000E+00	-9.655E-01	0.00E+00	-1.990E-01
114.82	0.887	0.805	-0.372	3.857E-01	-1.000E+00	-9.767E-01	0.00E+00	-1.912E-01
115.04	0.900	0.815	-0.381	3.844E-01	-1.000E+00	-9.879E-01	0.00E+00	-1.834E-01
115.25	0.912	0.825	-0.389	3.831E-01	-1.000E+00	-9.991E-01	0.00E+00	-1.756E-01
115.47	0.925	0.835	-0.398	3.818E-01	-1.000E+00	-1.010E-01	0.00E+00	-1.678E-01
115.68	0.938	0.845	-0.406	3.805E-01	-1.000E+00	-1.022E-01	0.00E+00	-1.600E-01
115.89	0.951	0.855	-0.415	3.792E-01	-1.000E+00	-1.034E-01	0.00E+00	-1.522E-01
116.10	0.963	0.865	-0.424	3.779E-01	-1.000E+00	-1.046E-01	0.00E+00	-1.444E-01
116.30	0.976	0.875	-0.433	3.766E-01	-1.000E+00	-1.058E-01	0.00E+00	-1.366E-01
116.51	0.989	0.885	-0.441	3.753E-01	-1.000E+00	-1.070E-01	0.00E+00	-1.288E-01
116.71	1.002	0.895	-0.450	3.740E-01	-1.000E+00	-1.082E-01	0.00E+00	-1.210E-01

# APPENDIX B

## FORTRAN PROGRAM

```

C*
C      PROGRAM FOR CALCULATING POTENTIAL FIELD IN AN AXISYMMETRIC
C      ELECTROSTATIC COLLECTOR, TAKING SPACE CHARGE INTO EFFECT.
C*      EXECUTIVE ROUTINE FOR PROCESSING MULTIPLE CASES
C*      AND MAIN CONTROL OF LOGICAL FLOW THROUGHOUT PROGRAM.
C*
C***
COMMON BO,CVF,DRHT(10),DRHM(16),DTHTD,DTHTR,DVDR(10),
1 DVDT(10),DVRDR,DVRDZ,EQL(10),ETA0,IBAR,IT,JF,JT,KPO,KPOI,
2 KPOSC,LOOP,NEQL,N1,N2,N3,PHD2A(10),PI,PI2,PSIA(10),PSIO(10),R,
3 RAD,RHM(17),RHOP(10),RHOPP(10),RHT(10),RHV(10),SPCH,TAU02,
4 THD(10),THMD(25),THSDEL,THSFAC,THSWHI,THSWLO,
5 THTD(10),THTR(10),TH1,TH2,V(17,25),VO,VR,
6 VSMI(10),VT(10),W(16),XCTR,XT(25,16),Y(16),ZJO
EQUIVALENCE (DTH,Y(1)),(TH,Y(2)),(RH,Y(3)),(RH2,RHP,Y(4)),
* (RH1P,Y(5)),(RH2P,Y(6)),(W(1),DELR),(W(2),AR),
* (W(3),Z),(W(4),Z2,ZP),(W(5),Z1P),(W(6),Z2P)

C***
C      SUBROUTINES-
C      1. MAIN
C      2. INPUT
C      3. INTGRN
C      4. DE
C      5. DERIV
C      6. RK
C      7. MESH
C      8. RZTRAJ
C      9. R7RK(RZDE)
C     10. RZDE
C     11. OUT
C     12. VFIELD
C     13. EQLINES
C     14. RHSCAL (A,ZJO,VO,TH1,THF,X,V2,IBAR,RHM,TH2)
C     15. PSICAL (R,Z,PSI,BO,ASM)
C     16. BRBZ (R,Z,BR,BZ,BO,ASM)

C
10 FORMAT(5HOPASS,13,1X,8HFOLLOWS-)

C
C      INITIALIZE SPACE CHARGE FIELD TO ZERO TO SET UP
C      LAPLACE EQUATION.
      DO 1 I=1,16
      DO 1 J=1,25
1 XT(J,I)=0.0

C
C      INITIALIZE MESH SIZE, BOUNDARY CONDITIONS, CONVERGENCE
C      CRITERIA.
PI=0.0
LKTR=1
CALL INPUT
L=LOOP

```

```

C
C      COMPUTE POTENTIAL FIELD FOR GIVEN SPACE CHARGE FIELD.
7 CALL VFIELD
  IF(SPCH.EQ.0.) GO TO 3
C
C      CONDITIONAL OUTPUT OF POTENTIAL FIELD.
  WRITE(6,10) LKTR
3 CALL OUT
C
C      INTEGRATION OF ELECTRON CLASS TRAJECTORIES THROUGH
C      THE COMPUTED POTENTIAL FIELD.
CALL INTGRN
L=L-1
LOOP=LOOP-1
JT=1
LKTR=LKTR+1
CALL INPUT
IF(L.GT.1) GO TO 2
C
  N1=2
  N2=8
  N3=1
  SPCH=0.0
  KPD=0
  IF(L.EQ.1) GO TO 2
C
  STOP
  END

```

#### SUBROUTINE INPUT

```

C*
C*      READS AND PRINTS INITIAL CONDITIONS, PARAMETERS AND
C*      MISCELLANEOUS DATA REQUIRED FOR INTERNAL USE BY
C*      PROGRAM (OUTPUT FREQUENCY, LOOPING INDICES, CONVERGENCE
C*      CRITERIA, ETC.).
C*
C***
COMMON B0,CVF,DRHT(10),DRHM(16),DTHTD,DTHTR,DVDR(10),
1 DVDT(10),DVRDR,DVRDZ,EQL(10),ETA0,IBAR,IT,JF,JT,KPD,KPOI,
2 KPOSC,LOOP,NEQL,N1,N2,N3,PHD2A(10),PI,PI2,PSIA(10),PSID(10),R,
3 RAD,RHM(17),RHOP(10),RHOPP(10),RHT(10),RHV(10),SPCH,TAUD2,
4 THD(10),THMD(25),THSDEL,THSFAC,THSWHI,THSWLO,
5 THTD(10),THTR(10),TH1,TH2,V(17,25),VO,VR,
6 VSM(10),VT(10),W(16),XCTR,XT(25,16),Y(16),ZJO
EQUIVALENCE (DTH,Y(1)),(TH,Y(2)),(RH,Y(3)),(RH2,RHP,Y(4)),
* (RH1P,Y(5)),(RH2P,Y(6)),(W(1),DELR),(W(2),AR),
* (W(3),Z),(W(4),Z2,ZP),(W(5),Z1P),(W(6),Z2P)
C***
16 FORMAT(2X,3HIO=,1PE13.3)
17 FORMAT(2X,3HJO=,1PE13.3,4X,5HR =,E10.3)
18 FORMAT(2X,3HVO=,1PE13.3,4X,5HBO =,E10.3)
19 FORMAT(2X,6HMGFA=,1PE10.3,4X,5HETA0=,E10.3)
20 FORMAT(2X,6HFO =,1PE10.3,4X,5HKP =,E10.3)
21 FORMAT(1X,6HINPUT-)
22 FORMAT(40I2)
23 FORMAT(16H BRILLOUIN FLOW.)

```



```

24 FORMAT(/1X,12HOUTPUT EVERY,12,1X,6HSTEPS.)
25 FORMAT(2X,6HTAU02=.E10,3,4X,5HRAD =,E10,3)
26 FORMAT(16F5,3)
27 FORMAT(3X,1H1,8X,4HDELI,9X,4HDELI,5X,5HTHETA,9X,3HVSM,
* 9X,7HVI,8X,6HINJEC.,8X,4HPSIO)
28 FORMAT(2X,12,2F13,3,F10,3,F12,3,1PE14,2,OPF10,3,1PE15,3)
29 FORMAT(16H0INITIAL VALUES-)
30 FORMAT(12X,5H(RAD),8X,5H(DEG),4X,5H(DEG),31X,6HANGLES)
31 FORMAT(1H1)
32 FORMAT(55H
33 FORMAT(8E10,3)
34 FORMAT(15H CCFINED FLOW.)
35 FORMAT(12,10F5,3)
36 FORMAT(/1X,29HCONE ANGLE IS OUT OF RANGE (=,F5,0,9H DEGREES))
37 FORMAT(/1X,30HSTEP SIZE TOO LARGE, DELTHETA=,F5,2)
38 FORMAT(/1X,32HCONFLICTING BOUNDARY CONDITIONS-)
39 FORMAT(2X,18HSURFACE POTENTIAL=,1PE9,2)
40 FORMAT(2X,15HBEAM POTENTIAL=,1PE9,2)
41 FORMAT(4F5,1)
42 FORMAT(24H0ND SPACE CHARGE EFFECTS)
43 FORMAT(1X,12,21H ITERATIONS FOR SPACE)
44 FORMAT(15H CHARGE EFFECTS)

```

```

C
C
C      INITIALIZE TRAJECTORY CALCULATIONS.
C      FIRST TIME SETTING OF INITIAL CONDITIONS, BOUNDARY
C      PARAMETERS, CONVERGENCE CRITERIA.

```

```

      JT=1
      IF(PI.NE.0.) GO TO 9

```

```

C
C      CONSTANTS.
      PI=3.14159265
      PI2=2.*PI
      CVF=180./PI
      F0=8.860E-14
      FTA0=1.753E+15
      OM=1.414E+10

```

```

C
C      READ/WRITE.
      WRITE(6,31)
      READ(5,32)
      WRITE(6,32)
      READ(5,33) R,RO,DTHTD,TH1
      READ(5,33) Z10,ZJ0,V0,DELR,CONFLO,RAD
      READ(5,22) NT,KPOI,N1,N2,N3,IBAR,LOOP,KPOSC

```

```

C
C      INCREASE STEP SIZE DTH, BY A FACTOR
C      OF (THSFAC) EVERY (THSDEL) DEGREES
C      IN THE THETA(5) RANGE FROM (THSWHI)
C      TO (THSWLO) DEGREES.
      READ(5,41) THSFAC,THSDEL,THSWHI,THSWLO
      READ(5,26) (VSMI(I), I=1,NT)
      READ(5,35) NFQL, (EQL(I), I=1,NEQL)
      TH2=177.-TH1/60.
      JF=25
      KPO=0
      ZKP=710/(V0*.1.5)

```

```

C

```

```

C      TEST MAGNITUDE OF CURRENT DENSITY
C      TO SEE IF SPACE CHARGE CALCULATIONS
C      SHOULD BE MADE.
      SPCH=0.0
      IF(7JO.LT.10.0) GO TO 14
      SPCH=1.0
      WRITE(6.43) LOOP
      WRITE(6.44)
      GO TO 15
14  WRITE(6.42)
15  TAU02=(R*R)/(2.*ETA0*V0)

C
C      INDICATE TYPE OF FLOW.
      IF(CONFLO.F0.0.0) GO TO 1
      WRITE(6.34)
      GO TO 2
1  WRITE(6.23)
2  CONTINUE

C
C      READ BOUNDARY CONDITIONS.
      READ(5.26) (XT(J.16), J=1,JF)
      DO 3 J=1,JF
3  XT(J.16)=-XT(J.16)
      XCTR=XT(1.16)
      DO 4 I=1.15
4  XT(1,I)=XCTR

C
C      INPUT DATA CHECK.
      IF(TH1.GE.0.0.AND.TH1.LE.174.) GO TO 5
      WRITE(6.36) TH1
      CALL EXIT
5  IF(DTHTD.LT.0.0.AND.DTHTD.GE.-.05) GO TO 6
      WRITE(6.37) DTHTD
      CALL EXIT
6  IF(VSMI(1).LE.ABS(XCTR)) GO TO 7
      T0=VSMI(NT)
      WRITE(6.38)
      WRITE(6.39) XCTR
      WRITE(6.40) T0
      CALL EXIT

C
C      INITIAL OUTPUT.
7  WRITE(6.21)
      WRITE(6.20) E0.ZKP
      WRITE(6.19) CM.ETA0
      WRITE(6.16) Z10
      WRITE(6.17) 7JO.R
      WRITE(6.18) V0.80
      WRITE(6.25) TAU02.RAD
      WRITE(6.24) KPOI
      DTHTR=DTHTD/CVF

C
C      DETERMINE ENTRY CONDITIONS.
      DIMENSION ALPH(10),DELI(10)
      T0=RAD/FLOAT(NT-1)
      DO 8 I=1,NT
      T1=FLOAT(I-1)*T0
      DELI(I)=ARSIN(T1/R)

```

```

      ALPH(I)=1.0*FLOAT(I)
      T2=PI-DELI(I)
      ST=SIN(T2)
      CT=COS(T2)
      ARE=R*ST
      ZED=R*(1.0+CT)
      CALL PSICAL(ARE,ZED,PSI,80,RAD)
      PSIO(I)=PSI
      IF(CONFLO.EQ.0.) PSIO(I)=0.0
8 CONTINUE

```

```

C
C      SETTING OF RHO-THETA VARIABLE MESH.
      CALL MESH
C
C      SPREAD INITIAL TRAJECTORY VALUES.
C
C      EVERY TIME INITIALIZATION OF TRAJECTORIES.

```

```

9 DO 10 IT=2,NT
  RHT(IT)=.9999
  ALPHA=ALPH(IT)/CVF
  GAMMA=PI-ALPHA-DELI(IT)+DTHTR
  T2=-RHT(IT)/(DTHTR*SIN(GAMMA))
  T3=SIN(ALPHA+DELI(IT))-SIN(GAMMA)
  RH2P=-T2*T3
  DRHT(IT)=RH2P
  RHOP(IT)=RH2P
10 THD(IT)=VSMI(IT)/(1.+RHOP(IT)**2)

```

```

C
C      CALCULATE VT(I).
      DO 11 I=1,NT
        THTR(I)=PI-DELI(I)
        THTD(I)=THTR(I)*CVF
11 VT(I)=V0*VSMI(I)

```

```

C
C      PRINT INITIAL TRAJECTORY VALUES.

```

```

      WRITE(6,29)
      WRITE(6,27)
      WRITE(6,30)
      DO 12 I=2,8
        DELID=DELI(I)*CVF
        T1=180.-DELI(I)
12 WRITE(6,28)I,DELI(I),DELID,T1,VSMI(I),VT(I),ALPH(I),PSIO(I)

```

```

C
      DO 13 I=2,NT
        IT=I
        TH=THTR(IT)
        RH=RHT(IT)
        RHP=RHOP(IT)
        CALL DE
13 RHOPP(IT)=RH2P

```

```

C
      RETURN
      END

```

# SUBROUTINE INTGRN

```

C*
C*      CONTROLS INTEGRATION LOOPING OF EQUATIONS OF MOTION,
C*      STEP-SIZE, CHANGEVER OF COORDINATE SYSTEMS AND THE
C*      NUMBER OF ITERATIONS REQUIRED FOR CONVERGENT SOLUTION.
C*
C***
      COMMON RD,CVF,DRHT(10),DRHM(16),DTHTD,DTHTR,DVDR(10),
1  DVDT(10),DVRDR,DVRDZ,EQL(10),ETA0,IBAR,IT,JF,JT,KPO,KPOI,
2  KPOSC,LOOP,AEQL,N1,N2,N3,PHD2A(10),PI,PI2,PSIA(10),PSID(10),R,
3  RAD,RHM(17),RHOP(10),RHOPP(10),RHT(10),RHV(10),SPCH,TAU02,
4  THD(10),THMC(25),THSDEL,THSFAC,THSWHI,THSWLO,
5  THTD(10),THTR(10),TH1,TH2,V(17,25),VO,VR,
6  VSMI(10),VT(10),W(16),XCTR,XT(25,16),Y(16),ZJC
      EQUIVALENCE (DTH,Y(1)),(TH,Y(2)),(RH,Y(3)),(RH2,RHP,Y(4)),
      * (RH1P,Y(5)),(RH2P,Y(6)),(W(1),DELR),(W(2),AR),
      * (W(3),Z),(W(4),Z2,ZP),(W(5),Z1P),(W(6),Z2P)
C***
10  FORMAT(7H0DT+TD=.1PE9.2)
      EXTERNAL DE
      DTH=DTHTR
C
C      CHECK FOR SPACE CHARGE ITERATION.
      IF(SPCH.EQ.0.) GO TO 1
      N1=5
      N2=5
      N3=1
      IF(LSW.EQ.9) GO TO 1
      LSW=9
      THD=THTD(5)
C
1  DO 2 IT=N1,N2,N3
      TH =THTR(IT)
      RH =RHT(IT)
      RHP=DRHT(IT)
      RGLD=RH
      CALL RK(DE)
      RHOP (IT)=RHP
      RHOPP(IT)=RH2P
      THTR(IT)=TH
      THTD(IT)=THTR(IT)*CVF
      RHT(IT)=RH
2  DRHT(IT)=RHP
C
C      INCREASE STEP SIZE DTH, BY A FACTOR
C      OF (THSFAC) EVERY (THSDEL) DEGREES
C      IN THE THETA(5) RANGE FROM (THSWHI)
C      TO (THSWLO) DEGREES.
      IF(THTD(5).GT.THSWHI) GO TO 3
      IF(THTD(5).LE.THSWLO) THSWHI=0.0
      THSWHI=THSWHI-THSDEL
      DTH=THSFAC*DTH
      T1=CVF*DTH
      WRITE(6,10) T1
C
3  CONTINUE
      JT=JT+1
      CALL OUT
      IF(SPCH.EQ.0.) GO TO 4
      IF(RH.GT.RHM(7)) GO TO 1

```

```

THF=THTD(5)
CALL RHSCAL(RAD,ZJO,VO,THO,THF,XT,VSMI,IBAR,RHM,THMD(1),KPOSC)
KPG=0
RETURN

```

```

C
C      R-7 COORDINATE TEST.
4 IF(THTR(2).GT.3.1) GO TO 5
  IF(RHOP(N2).LT.0.) CALL RZTRAJ
5 IF(RHT(N1).GT.1.0) GO TO 6
  GO TO 1
C
6 RETURN
END

```

# SUBROUTINE DE

```

C*
C*      CONTAINS EQUATIONS OF MOTION IN SPHERICAL
C*      COORDINATE SYSYTEM.
C*
C***

```

```

COMMON BO,CVF,DRHT(10),DRHM(16),DTHTD,DHTR,DVDR(10),
1 DVDT(10),DVRDR,DVRDZ,EOL(10),ETA0,IBAR,IT,JF,JT,KPO,KPOI,
2 KPOSC,LOOP,NEQL,N1,N2,N3,PHD2A(10),PI,PI2,PSIA(10),PSIO(10),R,
3 RAD,RHM(17),RHOP(10),RHOPP(10),RHT(10),RHV(10),SPCH,TAU02,
4 THD(10),THMD(25),THSDEL,THSFAC,THSWHI,THSWLO,
5 THTD(10),THTR(10),TH1,TH2,V(17,25),VO,VR,
6 VSMI(10),VT(10),W(16),XCTR,XT(25,16),Y(16),ZJO
EQUIVALENCE (DTH,Y(1)),(TH,Y(2)),(RH,Y(3)),(RH2,RHP,Y(4)),
* (RH1P,Y(5)),(RH2P,Y(6)),(W(1),DELR),(W(2),AR),
* (W(3),Z1),(W(4),Z2,ZP),(W(5),Z1P),(W(6),Z2P)

```

```

C***
      ST=SIN(TH)
      ST2=ST**2
      CT=COS(TH)

```

```

C
C      COMPUTE DV/DRHO AND DV/DTHETA.
CALL DERIV
ARE=RH*R*ST
ZED=R*(1.+RH*CT)

```

```

C
C      COMPUTE PSI.
CALL PSICAL(ARE,ZED,PSI,BO,RAD)

```

```

C
C      COMPUTE BR AND BZ.
CALL BRHZ(ARE,ZED,BR,BZ,BO,RAD)
T1=-ETA0/(ARE*ARE*PI2)
PHD=T1*(PSI-PSIO(IT))
PHD2=PHD**2
PHD2A(IT)=PHD2
PSIA(IT)=PSI

```

```

C
C      COMPUTES FIRST AND SECOND DERIVATIVES OF RHO WITH
C      RESPECT TO THETA (SPHERICAL COORDINATES).
DVMDRH=R*(BR*ST+BZ*CT)
DVMDTH=RH*R*(BR*CT-BZ*ST)
T1=RH*RH*R2*R*ST*PHD

```

```

PAR1=DVDR(IT)/R+ST*PHD*DVMDTH
PAR2=DVDT(IT)/R-T1*DVMDRH
T0=(VSM(IT)+VT(IT))/(TAUG2*RH*RH*(1.+(RHP/RH)**2))
THD2=T0-(PHD2*ST2)/(1.+(RHP/RH)**2)
THD(IT)=THD2
T1=RH*ST*PHC
T2=(T1*ST*PHD)/THD2
T5=ETA0/R
T3=T5/THD2
T1=RH+T2+T3*PAR1
T2=-(RHP*ST*CT*PHD2)/THD2
T3=(2.*RHP**2)/RH
T4=-(RHP*T5)/(RH*RH*THD2)
RH2P=T1+T2+T3+T4*PAR2
RH1P=RH2

```

```

C
RETURN
END

```

#### SUBROUTINE DERIV

```

C*
C*      CALCULATES THE RATES OF CHANGE OF THE POTENTIAL
C*      FIELD IN SPHERICAL COORDINATES FOR ANY SPECIFIED
C*      INTERIOR POINT.
C*
C***
COMMON B0,CVF,DRHT(10),DRHM(16),DTHD,DTHTR,DVDR(10),
1 DVDT(10),DVDRD,DVDRZ,EQL(10),ETA0,IBAK,IT,JF,JT,KPO,KPOI,
2 KPOSC,LOOP,NEQL,N1,N2,N3,PHD2A(10),PI,PI2,PSIA(10),PSIO(10),R,
3 RAD,RHM(17),RHOP(10),RHOPP(10),KHT(10),RHV(10),SPCH,TAUD2,
4 THD(10),THMD(25),THSDEL,THSFAC,THSWHI,THSWLO,
5 THTD(10),THTR(10),TH1,TH2,V(17,25),V0,VR,
6 VSMI(10),VT(10),W(16),XCTR,XT(25,16),Y(16),ZJO
EQUIVALENCE (DTH,Y(1)),(TH,Y(2)),(RH,Y(3)),(RH2,RHP,Y(4)),
* (RH1P,Y(5)),(RH2P,Y(6)),(W(1),DELR),(W(2),AR),
* (W(3),Z1),(W(4),Z2,ZP),(W(5),Z1P),(W(6),Z2P)

```

```

C***
T2=TH*CVF
T3=15.

C
C      DETERMINE RHO INTERPOLATION FACTOR (FR).
DO 1 I=1,17
IF(RHM(I).GT.RH) GO TO 2
1 CONTINUE
2 IF(I.EQ.17) I=16
FR=(RH-RHM(I-1))/DRHM(I-1)

C
C      DETERMINE THETA INTERPOLATION FACTOR (FT).
DO 3 J=1,25
IF(THMD(J).GT.T2) GO TO 4
3 CONTINUE
4 IF(T2.GT.TH2) T3=.25
FT=(T2-THMD(J-1))/T3
T3=T3/CVF

C
VP1=V(I-1,J-1)+FT*(V(I-1,J)-V(I-1,J-1))
VP2=V(I,J-1)+FT*(V(I,J)-V(I,J-1))

```

```

VP3=V(I-1,J )+FR*(V(I ,J )-V(I-1,J ))
VP4=V(I-1,J-1)+FR*(V(I ,J-1)-V(I-1,J-1))

```

C

```

VT(IT)=VP1+FR*(VP2-VP1)

```

C

```

EVALUATES DV/DRHO AND DV/DTHETA AT (RH,T2) FROM CURRENT
POTENTIAL FIELD.

```

C

```

DVDR(IT)=(VF2-VP1)/DRHM(I-1)*VG

```

```

DVDI(IT)=(VF3-VP4)/T3*V0

```

```

IF(THD(IT).GT.TH2) DVDI(IT)=0.0

```

C

```

RETURN

```

```

END

```

```

SUBROUTINE RK(DE)

```

C\*

C

```

INTEGRATES ONE TRAJECTORY ONE STEP USING RUNGE-KUTTA
FORMULAS IN SPHERICAL COORDINATES.

```

C\*

C\*\*\*

```

COMMON RD,CVF,DRHT(10),DRHM(16),DTHTD,DTHTR,DVDR(10),
1 DVDI(10),DVRDR,DVRDZ,EQL(10),ETA0,IBAR,IT,JF,JT,KPO,KPOI,
2 KPOSC,LNOP,NEQL,N1,N2,N3,PHD2A(10),PI,PI2,PSIA(10),PSID(10),R,
3 RAD,RHM(17),RHOP(10),RHOPP(10),RHT(10),RHV(10),SPCH,TAUD2,
4 THD(10),THMC(25),THSDEL,THSFAC,THSWHL,THSWLO,
5 THTD(10),THTR(10),TH1,TH2,V(17,25),V0,VR,
6 VSMI(10),VT(10),W(16),XCTR,XT(25,16),Y(16),ZJO
EQUIVALENCE (DTH,Y(1)),(TH,Y(2)),(RH,Y(3)),(RH2,RHP,Y(4)),
* (RH1P,Y(5)),(RH2P,Y(6)),(W(1),DELR),(W(2),AR),
* (W(3),Z),(W(4),Z2,ZP),(W(5),Z1P),(W(6),Z2P)

```

C\*\*\*

```

Y(15)=Y(3)

```

```

Y(16)=Y(4)

```

```

CALL DE

```

```

Y(7)=Y(1)*Y(5)

```

```

Y(8)=Y(1)*Y(6)

```

```

Y(2)=Y(2)+Y(1)/2.

```

```

Y(3)=Y(15)+.5*Y(7)

```

```

Y(4)=Y(16)+.5*Y(8)

```

```

CALL DE

```

```

Y(9)=Y(1)*Y(5)

```

```

Y(10)=Y(1)*Y(6)

```

```

Y(3)=Y(15)+.5*Y(9)

```

```

Y(4)=Y(16)+.5*Y(10)

```

```

CALL DE

```

```

Y(11)=Y(1)*Y(5)

```

```

Y(12)=Y(1)*Y(6)

```

```

Y(2)=Y(2)+Y(1)/2.

```

```

Y(3)=Y(15)+Y(11)

```

```

Y(4)=Y(16)+Y(12)

```

```

CALL DE

```

```

Y(13)=Y(1)*Y(5)

```

```

Y(14)=Y(1)*Y(6)

```

C

```

Y(3)=Y(15)+(Y(7)+2.*Y(9)+2.*Y(11)+Y(13))/6.

```

```

Y(4)=Y(16)+(Y(8)+2.*Y(10)+2.*Y(12)+Y(14))/6.

```

```

CALL DE
RETURN
END

```

# SUBROUTINE MESH

```

C*
C*   FOR ANY SPECIFIED COLLECTOR GEOMETRY, GENERATES
C*   GRADUATED MESH POINT ARRAYS IN BOTH THE RHO AND
C*   THETA DIRECTIONS.
C*
C***
COMMON B0,CVF,DRHT(10),DRHM(16),DTHD,DTHTR,DVDR(10),
1 DVDT(10),DVRDR,DVRDZ,EUL(10),ETA0,IBAR,IT,JF,JT,KPO,KPO1,
2 KPOSC,LGOP,NEQL,N1,N2,N3,PHD2A(10),PI,PI2,PSIA(10),PSID(10),R,
3 RAD,RHM(17),RHOP(10),RHOPP(10),RHT(10),RHV(10),SPCH,TAUD2,
4 THD(10),THMD(25),THSDEL,THSFAC,THSWHI,THSWLO,
5 THTD(10),THTR(10),TH1,TH2,V(17,25),VO,VR,
6 VSMI(10),VT(10),W(16),XCTR,XT(25,16),Y(16),ZJC
EQUIVALENCE (DTH,Y(1)),(TH,Y(2)),(RH,Y(3)),(RH2,RHP,Y(4)),
* (RH1P,Y(5)),(RH2P,Y(6)),(W(1),DELR),(W(2),AR),
* (W(3),Z),(W(4),Z2,ZP),(W(5),Z1P),(W(6),Z2P)
C***
C   GENERATE RHO AND DELRHO ARRAYS.
T1=0.8/120.
RHM(17)=1.0
C
C   GENERATE VARIABLE MESH RHO IN RHM ARRAY RANGING FROM
C   RHM(1)=0 TO RHM(17)=1 WITH FINE STEP AT END.
DO 1 I=1,16
J=17-I
DRHM(J)=FLOAT(I)*T1
1 RHM(J)=RHM(J+1)-DRHM(J)
DRHM(1)=0.2
RHM(1)=0.0
C
C   GENERATE THETA ARRAY.
JR=TH1/15.
JK=12-JK
C
C   GENERATE VARIABLE MESH THETA IN DEGREES IN THMD ARRAY
C   RANGING FROM THMD(1)=TH1 TO THMD(25)=180 WITH FINE STEP
C   AT END.
DO 2 J=1,JK
2 THMD(J)=TH1+15.*FLOAT(J-1)
JK1=JK+1
JK2=JK+2
THMD(JK1)=177.-.25*FLOAT(JR)
TH2=THMD(JK1)
DO 3 J=JK2,JF
3 THMD(J)=THMD(JK1)+.25*FLOAT(J-JK1)
RETURN
END

```



# SUBROUTINE RZTRAJ

```
C*
C*   CONTROLS INTEGRATION OF EQUATIONS OF MOTION IN THE
C*   R-Z RECTILINEAR COORDINATE SYSTEM.
C   COVERT FROM SPHERICAL COORDINATES (RHO,THETA) TO CYLINDRICAL
C   COORDINATES (R,Z) AND CONTINUE INTEGRATION OF TRAJECTORY UNTIL
C   IT REACHES SPHERICAL SURFACE.
```

C\*

C\*\*\*

```
COMMON R0,CVF,DRHT(10),DRHM(16),DTHTD,OTHTR,DVDR(10),
1 DVDT(10),DVRDR,DVRDZ,EQL(10),ETA0,IBAR,IT,JF,JT,KPD,KPOI,
2 KPOSC,LOOP,NEQL,N1,N2,N3,PHD2A(10),PI,PI2,PSIA(10),PSIO(10),R,
3 RAD,RHM(17),RHOP(10),RHOPP(10),RHT(10),RHV(10),SPCH,TAUC2,
4 THD(10),THMD(25),THSDEL,THSFAC,THSWHI,THSWLO,
5 THTD(10),THTR(10),TH1,TH2,V(17,25),VO,VR,
6 VSMI(10),VT(10),W(16),XCTR,XT(25,16),Y(16),ZJO
EQUIVALENCE (OTH,Y(1)),(TH,Y(2)),(RH,Y(3)),(RH2,RHP,Y(4)),
* (RH1P,Y(5)),(RH2P,Y(6)),(W(1),DELR),(W(2),AR),
* (W(3),Z),(W(4),Z2,ZP),(W(5),Z1P),(W(6),Z2P)
```

C\*\*\*

```
10 FORMAT(33H1SWITCH TO R-Z COORDINATE SYSTEM-)
11 FORMAT(15H TRAJECTORY NO.,I3,2X,5HDELR=,F4.3)
12 FORMAT(/4X,5HTHETA,3X,3HRHO,5X,1HR,7X,1HZ,6X,4HDVDR,8X,4HDVDZ,9X,
* 2HZP,10X,3HZPP,10X,1HV)
13 FORMAT(2X,F7.2,3F7.3,1P5E12.3)
```

C

```
EXTERNAL RZDE
WRITE(6,10)
WRITE(6,11) N2,DELR
WRITE(6,12)
```

C

C CONVERT TO R-Z COORDINATES.

```
AR=RHT(N2)*SIN(TH)
Z =RHT(N2)*COS(TH)
```

C

C INITIALIZE R-Z INTEGRATION.

```
T0=RHOP(N2)*Z-RHT(N2)*AR
T1=RHT(N2)*Z+RHOP(N2)*AR
ZP=T0/T1
CALL RZDE
THRZ=90.-CVF*ATAN(Z/AR)
RHRZ=SQRT(AR*AR+Z*Z)
T2=DVRDZ-ZP*DVRDR
T0=VSMI(IT)+VR
T1=1.+ZP**2
T3=2.*(T0/T1)
Z2P=T2/T3
WRITE(6,13) THRZ,RHRZ,AR,Z,DVRDR,DVRDZ,ZP,Z2P,VR
```

C

C INTEGRATE TO SURFACE.

```
1 CALL RZRK(RZDE)
THRZ=90.-CVF*ATAN(Z/AR)
RHRZ=SQRT(AR*AR+Z*Z)
WRITE(6,13) THRZ,RHRZ,AR,Z,DVRDR,DVRDZ,ZP,Z2P,VR
IF(RHRZ.LT.1.0) GO TO 1
IF(N1.EQ.N2) T0=T0/0.0
```

C

```
N2=N2-1
RETURN
END
```

SUBROUTINE RZRK(RZDE)

```

C*
C
C      INTEGRATES ONE TRAJECTORY ONE STEP USING RUNGE-KUTTA
C      FORMULAS IN CYLINDRICAL COORDINATES.
C*
C***
COMMON B0,CVF,DRHT(10),DRHM(16),DTHTD,DTHTR,DVDR(10),
1 DVT(10),DVRDR,DVRDZ,EQL(10),ETA0,IBAR,IT,JF,JT,KPO,KPOI,
2 KPOSC,LOOP,NEQL,N1,N2,N3,PHD2A(10),PI,PI2,PSIA(10),PSIO(10),R,
3 RAD,RHM(17),RHOP(10),RHOPP(10),RHT(10),RHV(10),SPCH,TAU02,
4 THD(10),THMD(25),THSDEL,THSFAC,THSWHI,THSWLO,
5 THTD(10),THTR(10),TH1,TH2,V(17,25),VO,VR,
6 VSMI(10),VT(10),W(16),XCTR,XT(25,16),Y(16),ZJC
EQUIVALENCE (DTH,Y(1)),(TH,Y(2)),(RH,Y(3)),(RH2,RHP,Y(4)),
* (RH1P,Y(5)),(RH2P,Y(6)),(W(1),DELK),(W(2),AR),
* (W(3),Z),(W(4),Z2,ZP),(W(5),Z1P),(W(6),Z2P)

```

```

C***
W(15)=W(3)
W(16)=W(4)
CALL RZDE
W(7)=W(1)*W(5)
W(8)=W(1)*W(6)
W(2)=W(2)+W(1)/2.
W(3)=W(15)+.5*W(7)
W(4)=W(16)+.5*W(8)
CALL RZDE
W(9)=W(1)*W(5)
W(10)=W(1)*W(6)
W(2)=W(15)+.5*W(9)
W(4)=W(16)+.5*W(10)
CALL RZDE
W(11)=W(1)*W(5)
W(12)=W(1)*W(6)
W(2)=W(2)+W(1)/2.
W(3)=W(15)+W(11)
W(4)=W(16)+W(12)
CALL RZDE
W(13)=W(1)*W(5)
W(14)=W(1)*W(6)
W(3)=W(15)+(W(7)+2.*W(9)+2.*W(11)+W(13))/6.
W(4)=W(16)+(W(8)+2.*W(10)+2.*W(12)+W(14))/6.
CALL RZDE
RETURN
END

```

SUBROUTINE RZDE

```

C
C      COMPUTES FIRST AND SECOND DERIVATIVES OF Z WITH
C      RESPECT TO R (CYLINDRICAL COORDINATES).
C*
C***
COMMON B0,CVF,DRHT(10),DRHM(16),DTHTD,DTHTR,DVDR(10),
1 DVT(10),DVRDR,DVRDZ,EQL(10),ETA0,IBAR,IT,JF,JT,KPO,KPOI,
2 KPOSC,LOOP,NEQL,N1,N2,N3,PHD2A(10),PI,PI2,PSIA(10),PSIO(10),R,
3 RAD,RHM(17),RHOP(10),RHOPP(10),RHT(10),RHV(10),SPCH,TAU02,

```

```

4 THD(10).THMC(25).THSDEL.THSFAC.THSWHI.THSWLO,
5 THTD(10).THTR(10).TH1.TH2.V(17,25).VO.VR,
6 VSMI(10).VT(10).W(16).XCTR.XT(25,16).Y(16).ZJC
EQUIVALENCE (DTH,Y(1)).(TH,Y(2)).(RH,Y(3)).(RH2,RHP,Y(4)),
* (RH1P,Y(5)).(RH2P,Y(6)).(W(1),DELR).(W(2),AR),
* (W(3),Z1).(W(4),Z2,ZP).(W(5),Z1P).(W(6),Z2P)
C***
  RH=SQRT(Z**2+AR**2)
  TH=ATAN2(AR,Z)
  CALL DERIV
  VR=VT(IT)
  DVDR=(AR*DVER(IT)+(Z*DVDIT(IT))/RH)/(RH*VO)
  DVRDZ=(Z*DVR(IT)-AR*DVDIT(IT))/RH/(RH*VO)
  T1=DVRDZ-ZP*DVR
  T2=2.*((VSMI(IT)+VR)/(1.+ZP**2))
  Z2P=T1/T2
  Z1P=Z2
C
  RETURN
END

SUBROUTINE OUT
C*
C  PRINTS OUT SELECTED DATA ALONG A TRAJECTORY.
C*
C***
  COMMON B0,CVF,DRHT(10),DRHM(16),DTHTD,DTHTR,DVDR(10),
1 DVDT(10),DVRDR,DVRDZ,EQL(10),ETA0,IBAR,IT,JF,JT,KPO,KPOI,
2 KPOSC,LOOP,NEQL,N1,N2,N3,PHD2A(10),PI,PI2,PSIA(10),PSID(10),R,
3 RAD,RHM(17),RHOP(10),RHOPP(10),RHT(10),RHV(10),SPCH,TAU02,
4 THD(10).THMC(25).THSDEL.THSFAC.THSWHI.THSWLO,
5 THTD(10).THTR(10).TH1.TH2.V(17,25).VO.VR,
6 VSMI(10).VT(10).W(16).XCTR.XT(25,16).Y(16).ZJC
EQUIVALENCE (DTH,Y(1)).(TH,Y(2)).(RH,Y(3)).(RH2,RHP,Y(4)),
* (RH1P,Y(5)).(RH2P,Y(6)).(W(1),DELR).(W(2),AR),
* (W(3),Z1).(W(4),Z2,ZP).(W(5),Z1P).(W(6),Z2P)
C***
C  FORMAT STATEMENTS.
10 FORMAT(10HDELTHETA=,F7.4,5H DEG.)
11 FORMAT(5H STEP,I5)
12 FORMAT(/1X,3FTRJ,2X,5HTHETA,2X,3HRHO,6X,
A 2HVT,7X,5HDVDRH,7X,5HDVDTH,6X,5HRH-PR,6X,6HRH-PPR,6X,4HTHD2,
B 6X,4HPHD2,6X,3HPSI)
13 FORMAT(1X,I2,F8.2,F6.3,1P8E11.3)
C
C  PRINT TITLES.
  IF(K9.EQ.9) GO TO 1
  K9=9
  WRITE(6,10) DTHTD
  WRITE(6,12)
C
1  IF(KPO.GT.1) GO TO 4
  JT1=JT-1
  WRITE(6,11) JT1
  DO 2 I=N1,N2,N3

```

```

2 WRITE(6,13) I,THTD(I),RHT(I),VT(I),DVDR(I),
* DVDT(I),RPOP(I),RHOPP(I),THD(I),PHD2A(I),PSIA(I)
IF(RHT(N2).GT.1.0) GO TO 3

```

C

```

KPC=KPOI
RETURN
3 N2=N2-1
KPC=KPOI
RETURN
4 KPC=KPO-1
IF(RHT(N2).GE.1.0) GO TO 4
RETURN
END

```

#### SUBROUTINE VFIELD

```

C*
C
C      COMPUTES THE POTENTIAL FIELD V FOR A GIVEN SPACE CHARGE
C      FIELD BY SOLVING POISSONS EQUATION.
C
C      POISS1 AND POISS2 ARE SUBROUTINES DESCRIBED BY THE TN
C      OF REFERENCE 2. THEY WERE DEVELOPED TO SOLVE POISSONS
C      EQUATION IN A SUBREGION OF A SPHERE IN AN EFFICIENT
C      NON-ITERATIVE FASHION. USING A BLOCK DIAGONAL MATRIX
C      TECHNIQUE.
C*

```

```

COMMON/BLOCK1/NR,NT,RA(17),TA(25),X(25,16),X1,AVS

```

C\*\*\*

```

COMMON RO,CVF,DRHT(10),DRHM(16),DTHTD,DTHTR,DVDR(10),
1 DVDT(10),DVRDR,DVRDZ,EQL(10),ETA0,IBAR,IT,JF,JT,KPO,KPOI,
2 KPOSC,LOOP,NEQL,N1,N2,N3,PHD2A(10),PI,PI2,PSIA(10),PSID(10),R,
3 RAD,RHM(17),RHOP(10),RHOPP(10),RHT(10),RHV(10),SPCH,TAU02,
4 THD(10),THMD(25),THSDEL,THSFAC,THSWHI,THSWLO,
5 THTD(10),THTR(10),TH1,TH2,V(17,25),VO,VR,
6 VSMI(10),VT(10),W(16),XCTR,XT(25,16),Y(16),ZJO
EQUIVALENCE (DTH,Y(1)),(TH,Y(2)),(RH,Y(3)),(RH2,RHP,Y(4)),
* (RH1P,Y(5)),(RH2P,Y(6)),(W(1),DELR),(W(2),AR),
* (W(3),Z),(W(4),Z2,ZP),(W(5),Z1P),(W(6),Z2P)

```

C\*\*\*

```

LOGICAL AVS
DIMENSION XB(15),TD(25)

```

C

```

23 FORMAT(16F5.3)
24 FORMAT(1X,F6.2,1P12E10.2)
25 FORMAT(7H INPUT-.52X,3HRHO)
26 FORMAT(11H0**NO BAR**)
27 FORMAT(13H0 BAR VALUES-)
28 FORMAT(4X,1HR,8X,1HV)
29 FORMAT(2X,F5.3,3X,F6.3)
30 FORMAT(8H OUTPUT-.52X,3HRHO)
31 FORMAT(6H THETA,3X,16(F5.3,2X))
32 FORMAT(6H THETA,3X,12(F5.3,5X))
33 FORMAT(4H X1=.F5.2)
34 FORMAT(1X,F6.2,16F7.4)
35 FORMAT(/54X,15HPOTENTIAL FIELD)

```

```

C      X1=XCTR
      NR=17
      NR1=NR-1
      NR2=NR-2
      DO 1 I=1,17
1  RA(I)=RHM(I)
      NT=JF
      NT1=NT-1
      DO 2 J=1,NT
      DO 2 K=1,NR1
2  X(J,K)=XT(J,K)

C      IF AXIAL SPIKE IS PRESENT IN THIS PARTICULAR PROBLEM,
C      READ IN THESE VALUES AND DISPLAY THEM.
C      IF(IBAR.EQ.0) GO TO 4
      DO 3 I=1,NR2
3  X(NT,I)=XB(I)
4  DO 5 J=1,NT
      TD(J)=THMD(J)
5  TA(J)=THMD(J)/CVF
      IF(IBAR.EQ.0) GO TO 9

C      READ BAR VALUES.
C      AVS=.TRUE.
      IF(LSW.EQ.9) GO TO 7
      LSW=9
      READ(5,23) (X(NT,I), I=1,NR1)
      DO 6 I=1,NR2
      XB(I)=-X(NT,I)
6  X(NT,I)=-X(NT,I)

C      PRINT BAR VALUES.
C      7 WRITE(6,27)
      WRITE(6,28)
      WRITE(6,29) RA(1),X1
      DO 8 I=1,NR1
      J=I+1
8  WRITE(6,29) RA(J),X(NT,I)
      GO TO 10
9  AVS=.FALSE.
      WRITE(6,26)

C      SET-UP AND FACTOR SUB-MATRICES IN BLOCK DIAGONAL
C      COEFFICIENT MATRIX.
C      10 CALL POISS1

C      PRINT INPUT BLOCK.
C      WRITE(6,35)
      WRITE(6,25)
      WRITE(6,32) (RA(I), I=6,NR)
      DO 11 J=1,NT
11  WRITE(6,24) TD(J), (X(J,K-1), K=6,NR)
      WRITE(6,33) X1

C      CARRY OUT SOLUTION OF MATRIX PROBLEM TO YIELD V-FIELD.
C      CALL POISS2
C

```

```

C      ADJUST BAR VALUES.
      IF (IBAR.EQ.0) GO TO 17
      DO 16 I=4,16
16 X(NT,I)=X(NT1,I)
C
C      PRINT OUTPUT BLOCK.
17 WRITE(6,35)
   WRITE(6,30)
   WRITE(6,31) (RA(I), I=2,NR)
   DO 12 J=1,JF
12 WRITE(6,34) TD(J),(X(J,K-1),K=2,NR)
   DO 13 J=2,JF
   DO 13 K=1,15
13 XT(J,K)=X(J,K)
C
C      DISPLAY EQUIPOTENTIAL LINE DATA.
      IF (LOOP.LE.1) CALL EQLINE
      DO 14 J=1,JF
14 V(1,J)=XCTR
   DO 15 I=2,17
   K=I-1
   DO 15 J=1,JF
15 V(I,J)=XT(J,K)
C
      RETURN
      END

```

#### SUBROUTINE ECLINE

```

C*
C
C      FIND ON EACH THETA MESH LINE THE RHO VALUES ASSOCIATED
C      WITH NEQL PRE-SPECIFIED POTENTIAL VALUES. AN EQUIPOTENTIAL
C      CURVE PASSES THROUGH SETS OF THESE POINTS.
C*
C***
      COMMON R0,CVF,DRHT(10),DRHM(16),DTHD,DTHTR,DVDR(10),
1 DVDT(10),DVRDR,DVRDZ,EQL(10),ETA0,IBAR,IT,JF,JT,KPC,KPD1,
2 KPOSC,LOOP,NEQL,N1,N2,N3,PHD2A(10),PI,PI2,PSIA(10),PSIO(10),R,
3 RAD,RHM(17),RHOP(10),RHOPP(10),RHT(10),RHV(10),SPCH,TAU02,
4 THD(10),THMD(25),THSDEL,THSFAC,THSWHI,THSWLO,
5 THTD(10),THTR(10),TH1,TH2,V(17,25),VO,VR,
6 VSMI(10),VT(10),W(16),XCTR,XT(25,16),Y(16),ZJO
      EQUIVALENCE (DTH,Y(1)),(TH,Y(2)),(RH,Y(3)),(RH2,RHP,Y(4)),
* (RH1P,Y(5)),(RH2P,Y(6)),(W(1),DELR),(W(2),AR),
* (W(3),Z1),(W(4),Z2,ZP),(W(5),Z1P),(W(6),Z2P)
C***
10 FORMAT(/28X,23HTABLE OF RHO-VALUES FOR)
11 FORMAT(30X,19HEQUIPOTENTIAL LINES)
12 FORMAT(1X,F6.2,2X,10F10.3)
13 FORMAT(2X,5HTHETA,2X,10(F10.2))
C
C      ZERO OUT RHV-ARRAY.
      DO 6 I=1,10
6 RHV(I)=0.0
C
      WRITE(6,10)
      WRITE(6,11)

```

```

NR=17
WRITE(6,13) (EQL(I), I=1,NEQL)
C
DO 5 J=1,JF
DO 4 I=1,NEQL
DO 1 K1=1,NR
K=NR-K1
IF(EQL(I).GT.XT(J,K)) GO TO 2
1 CONTINUE
C
2 IF(K1.GT.1) GO TO 3
RHV(I)=0.0
GO TO 5
C
3 F=(XT(J,K)-EQL(I))/(XT(J,K)-XT(J,K+1))
IF(K.GT.0) GO TO 4
F=(XCTR-EQL(I))/(XCTR-XT(J,K+1))
4 RHV(I)=RHM(K+1)+F*(RHM(K+2)-RHM(K+1))
5 WRITE(6,12) THMD(J), (RHV(I), I=1,NEQL)
C
RETURN
END

```

SUBROUTINE RSCAL(A,ZJO,V0,TH0,THF,X,V2,IBAR,RHM,TH2,KPOSC)

```

C*
C    RIGHT-HAND SIDE CALCULATION FOR POISSON MATRIX EQUATION.
C    EQUIVALENT TO CALCULATION OF SPACE CHARGE FIELD.
C*
    DIMENSION V(11),C(9),VI(10),RH(11),AD(11),RHS(11,9),ARG(16),
*      THD(11,9),THR(11,9),RHSI(10,16),X(25,16),V2(10),RHM(17)
C
C    FORMAT STATEMENTS.
22 FORMAT(1X,F5.3,F7.3)
23 FORMAT(16F5.0)
24 FORMAT(11HORFS ARRAY-)
25 FORMAT(1X,16F8.1)
26 FORMAT(2X,16F8.2)
27 FORMAT(10F5.0)
28 FORMAT(/2X,3FRHO,5X,2H-V)
29 FORMAT(12HORFS VALUES.)
30 FORMAT(/2X,3FRHO,4X,1HC,2X,4HTUBE,4X,5HTHETA,6X,3HRHS)
31 FORMAT(1X,F5.3,2I4,1H-,11,F10.3,F9.1)
32 FORMAT(5H TH)=,F7.3,7X,5HTHF =,F8.3)
33 FORMAT(/4X,5HAXIAL/2X,9HPOTENTIAL/1X,12HDISTRIBUTION)
C
C    A=RADIUS OF ENTRY HOLE.
C    ZJO=JO (CURRENT DENSITY).
C    TH0=INITIAL VALUE OF TRAJECTORY 5.
C    X=XT(25,16), SOURCE TERMS.
C    V2=ENERGY CLASSES.
C    TH2=CONF ANGLE.
TH1=TH0
IF=11
JF= 7
JF1=JF+1
JF2=JF+2
ENT=8.

```

```

EO =8.860E-14
ETA=1.753E+15
C1 =2.*EO*SQRT(2.*ETA)*ENT*ENT
PI =3.14159265
CVF=180./PI
WRITE(6.29)
WRITE(6.32) THO,THF

C
C      SECTION FOR COMPUTING SPACE CHARGE ALONG
C      TUBE CENTER LINES.
C      I=BIG LOOP FOR 11 RHO VALUES FROM 0.63 TO 1.00
C      J=SM. LOOP FOR 7 TUBES (1-2,2-3,.....7-8).
C      THF=RHO .63 CROSSING ANGLE OF TRAJ. NO. 5.
C      READ 11 AXIAL V-VALUES(RHO .63 TO 1.0)
C      AND VSMI-ARRAY(9).
C
C      GENERATE ARG-ARRAY, C-ARRAY, AND VI-ARRAY.
C      ARG(K)=THETA MESH VALUES IN HOLE REGION.
C      C (J)=1,3,5,.....13 (MULTIPLIERS).
C      VI (J)=1.55,1.40,.....0.4,0.0 (ENERGY CLASSES IN TUBES).
DO 1 K=1,16
1 ARG(K)=180.-FLOAT(K)*.25
DO 2 J=1,JF
VI(J)=(V2(J)+V2(J+1))/2.
2 C(J)=2*J-1

C
C      GENERATE AND PRINT RH-ARRAY AND V-ARRAY.
C      RH(I) ARRAY-11 AXIAL RHO MESH VALUES
C      FROM .633 TO 1.000
C      V (I)-POTENTIAL DISTRIBUTION AT THESE
C      11 AXIAL MESH POINTS.
WRITE(6.33)
WRITE(6.28)
DO 3 I=1,IF
RH(I)=RHM(I+6)
V(I)=-X(25,I+5)
3 WRITE(6.22) RH(I),V(I)

C
C      GENERATE THETA-ARRAY AND SPREAD THROUGHOUT
C      SPACE CHARGE REGION (BASED ON TRAJECTORY NO. 5).
DTH=TH1-THF
ORD=1.-RHM(7)
TO=DTH/ORD
DO 5 I=1,IF
I6=I+6
DIFF=RHM(I6)-RHM(7)
T1=THF+TO*DIFF
T2=T1+(180.-T1)/8.
DEL=(180.-T2)/4.
DO 4 J=1,JF2
THD(I,J)=180.-FLOAT(J)*DEL
4 THR(I,J)=THD(I,J)/CVF
5 CONTINUE

C
C      GENERATE AD-ARRAY (DISTANCE BETWEEN
C      TRAJECTORIES 4 AND 5 AT EACH OF
C      11 RHO MESH LINES).
DO 6 I=1,IF
TX1=RH(I)*TAN(THR(I,5))
TX2=RH(I)*TAN(THR(I,4))

```



```

6 AD(I)=TX2-TX1
C
C      CALCULATE SOURCE TERMS FOR ALL TRAJECTORY
C      CROSSINGS OF RHO MESH LINES.
      AJ=A*A*ZJ0
      DO 9 I=1,IF
      IF(KPQSC.NE.0) WRITE(6,30)
      DO 9 J=1,JF
      E1=V(I,J)-V(I)
      IF(E1.GT.0.) GO TO 7
      RHS(I,J)=0.0
      GO TO 8
7 E2=SQRT(E1)
  ST=SIN(THR(I,J))
  DEN=C1*SQRT(V0**3)*E2*RH(I)*ST*AD(I)
  RHS(I,J)=(C(J)*AJ)/DEN
8  J1=J+1
  IC=C(J)
  IF(KPQSC.NE.0) WRITE(6,31) RH(I),IC,J,J1,THD(I,J),RHS(I,J)
9 CONTINUE
C
C      SECTION FOR INTERPOLATING SPACE CHARGE FIELD AT MESH POINTS.
      DO 15 I=1,10
      DO 15 K=1,16
      DO 10 J=1,7
      IF(ARG(K).GT.TH0(I,J)) GO TO 11
10 CONTINUE
11 IF(J.NE.1) GO TO 13
  DELRHS=0.-RHS(I,J)
  T1=180.-TH0(I,J)
12 T2=ARG(K)-TH0(I,J)
  F=T2/T1
  IF(ARG(K).LT.TH0(I,J)) GO TO 14
  T1=RHS(I,J)+F*DELRHS
  RHS(I,K)=(RHS(I,K)+T1)/2.
  GO TO 15
13 T1=TH0(I,J-1)-TH0(I,J)
  DELRHS=RHS(I,J-1)-RHS(I,J)
  GO TO 12
14 RHS(I,K)=0.0
15 CONTINUE
  IF(KPQSC.EQ.0) GO TO 17
C
C      PRINT.
      WRITE(6,24)
      WRITE(6,26) (ARG(K), K=1,16)
      DO 16 I=1,10
16 WRITE(6,25) (RHS(I,K), K=1,16)
C
C      ZERO OUT RHS PREPARATORY TO
C      LOADING SOURCE TERMS.
17 DO 18 J=2,24
  DO 18 K=1,15
18 X(J,K)=0.0
  IF(IBAR.NE.0) GO TO 20
  DO 19 I=1,16
19 X(25,I)=0.0

```

```

C
20 J2=13.-TH2/15.
   DO 21 J=J2,24
     DO 21 K=6,15
       J1=25-J
       K1=K-5
21 X(J,K)=RHSI(K1,J1)

```

```

C
   RETURN
   END

```

SUBROUTINE PSICAL(R,Z,PSI,B0,ASM)

```

C*
C*      CALCULATES PSI, THE MAGNETIC FLUX, OF THE MAGNETIC
C*      FIELD AT EACH MESH POINT IN THE REGION OF THE
C*      ENTRY HOLE.
C*

```

```

   PI=3.14159265
   RF=R
   RSQ=R*R
   X= Z/ASM
   X2 = X*X
   AT = ATAN2(ASM,-Z)

```

```

C
   T= 1.+X2
   T0 = PI-AT-X/T
   T4 = 3.-5.*X2
   T6= 3.-7.*X2*(2.-X2)
   T= 21.-5.*X2
   T= 15.-X2*T
   T8= 5.-3.*X2*T
   T= 36.-5.*X2
   T= 54.-X2*T
   T= 20.-X2*T
   T10=9.*(15.-11.*X2*T)
   T= 11.-X2
   T= 7.*X2*T
   T= 198.-T
   T= 154.-X2*T
   T= 35.-X2*T
   T12 = 21.-13.*X2*T

```

```

C
   X1= ASM*(1.+X2)
   V= (RF/X1)**2

```

```

C
   T= (21.*T10)/5.+(11.*T12*V)/4.
   T= 7.*T8+0.5*V*T
   T=(5.*T6)/3.+0.125*V*T
   T= T4/4.+0.125*V*T
   T= 1.+V*T
   T= T0-(ASM*X*RSQ*T)/(X1**3)
   PSI= B0*RSQ*T

```

```

C
   RETURN
   END

```

```

SUBROUTINE BFBZ(R,Z,BR,BZ,B0,ASM)
C*
C*      CALCULATES BR AND BZ, THE R AND Z COMPONENTS OF THE
C*      MAGNETIC FIELD AT EACH MESH POINT IN THE REGION
C*      OF THE ENTRY HOLE.
C*
PI=3.14159265
IF(Z.EQ.0.0) Z=.0004
X=Z/ASM
X2=X**2

C
T1=1.
T2=1.
T3=1.-5.*X2
T4=3.-5.*X2
T5=3.-7.*X2*(6.-5.*X2)
T6=3.-7.*X2*(2.-X2)
T7=1.-X2*(27.-7.*X2*(9.-3.*X2))
T8=5.-3.*X2*(15.-X2*(21.-5.*X2))
T9=30.-X2*(28.-5.*X2)
T9=5.-11.*X2*(20.-3.*X2*T9)
T10=54.-X2*(36.-5.*X2)
T10=20.-X2*T10
T10=9.*(15.-11.*T10*X2)

C
T11=18.-X2*(9.-X2)
T11=195.-143.*X2*(10.-X2*T11)
T11=3.-X2*T11
T12=-X2*(1001.-91.*X2)
T12=-X2*(2574.+T12)
T12=-X2*(2002.+T12)
T12=-X2*(455.+T12)
T12=11.*(21.+T12)
T1B=(ASM*Z)/(ASM*ASM+Z*Z)

C
ZK=1.+X2
A1=ASM*ZK
A2=ASM*ZK*X

C
C1=(-2.*B0)/(PI*ASM*ZK*ZK)
C2=(-4.*C1*X)/A1
C3=C2/A2
C4=(-6.*C3*X)/A1
C5=C4/A2
C6=(-40.*C5*X)/A1
C7=(3.*C6)/A2
C8=(-14.*C7*X)/A1
C9=C8/A2
C10=(-4.*C9*X)/A1
C11=(45.*C10)/A2
C12=(-2.*C11*X)/A1

C
AT=ATAN2(ASM,-Z)
BB=(B0/PI)*(PI-AT-T1B)
B 1=C 1*T 1
B 2=C 2*T 2
B 3=C 3*T 3
B 4=C 4*T 4
B 5=C 5*T 5
B 6=C 6*T 6

```

B 7=C 7\*T 7  
B 8=C 8\*T 8  
B 9=C 9\*T 9  
B10=C10\*T10  
B11=C11\*T11  
B12=C12\*T12

C

R2=R/2.  
RS=R2\*R2  
T1=B10-RS\*B12/36.  
T1=B8-RS\*T1/25.  
T1=B6-RS\*T1/16.  
T1=B4-RS\*T1/9.  
T1=B2-RS\*T1/4.  
BZ=B8-RS\*T1

C

T1=B9-B11\*RS/30.  
T1=B7-RS\*T1/20.  
T1=B5-RS\*T1/12.  
T1=B3-RS\*T1/6.  
T1=B1-RS\*T1/2.  
BR=-R2\*T1

C

RETURN  
END

## APPENDIX C

### FORTTRAN SYMBOLS

ALPH(10)	array of entry angles, $\alpha$ , rad
ALPHA	entry angle, $\alpha$ , deg
AR	rectilinear coordinate, r
ASM	radius of entry hole, a, cm
AVS	axial boundary value logical switch TRUE indicates presence of an axial spike
B0	magnetic flux density, $B_0$
BR	r-component of magnetic field, $B_r$
BZ	z-component of magnetic field, $B_z$
CONFLO	switch for type of flow (confined flow when not equal to 0; Brillouin flow when equal to 0)
CVF	conversion factor, deg to rad
DELI(10)	$\delta_i$ array, rad
DELID	entry angles of electron classes, $\delta_i$ , deg
DEL R	step size $\Delta r$ for r-z trajectory integration
DRHM(16)	$\Delta\rho$ of mesh
DRHT(10)	$\Delta\rho$ of trajectories
DTH	$\Delta\theta$ of trajectories (equivalent to DTHTR below), rad
DTHTD	$\Delta\theta$ of trajectories (step in $\theta$ for $\rho$ - $\theta$ trajectory integration), deg
DTHTR	$\Delta\theta$ of trajectories, rad
DVDR(10)	$\partial V/\partial\rho$ array
DVDT(10)	$\partial V/\partial\theta$ array
DVMDRH	$\partial V_m/\partial\rho$ array
DVMDTH	$\partial V_m/\partial\theta$
DVRDR	$\partial V_r/\partial r$
DVRDZ	$\partial V_r/\partial z$
EQL(10)	array of values for which equipotential lines are to be calculated

ETA0	initial electron charge-to-mass ratio
E0	permittivity of free space, $\epsilon_0$
FLOOP	storage for number of iteration loops in space charge calculation
IBAR	indicator for axial boundary values
IT	iteration counter
J1, J2, JF, JT	looping indexes
KPO, KPOI	main output frequency control of trajectory data (e.g., 5 means to print every fifth point); KPOI is constant; KPO may be varied
KPOSC	output control for space charge values
K9	initialization switch
LKTR	counter for number of loops
LOOP	indicator switch for space charge looping
NEQL	number of equipotential lines to be calculated
N1, N2, N3	control indexes for trajectory calculations
NF	number of $\theta$ -mesh lines, usually 26
NR	number of $\rho$ -mesh points, usually 17
NT	number of trajectories, usually 9
PHD	$\dot{\varphi}(\partial\varphi/\partial t)$ , where $\varphi$ is azimuthal angle
PHD2	$\dot{\varphi}^2$
PHD2A(10)	$\dot{\varphi}^2$ array for output
PI, PI2	$\pi, \pi^2$
PSI	magnetic flux, $\psi$
PSIA(10)	$\psi$ array
PSI0	initial magnetic flux, $\psi_0$
R	radius of collector, R, cm
RA(17)	array of r-mesh values
RAD	radius of entry hole, a, cm
RH, RHP	$\rho, \rho'(\partial\rho/\partial\theta)$
RH1P	$\rho'_1$
RH2, RH2P	$\rho_2, \rho'_2$

RHM(17)	$\rho$ -mesh values
RHOP(10)	$\rho'$
RHOPP(10)	$\rho''$
RHRZ	$\rho$ in r-z coordinate system
RHT(10)	$\rho$ -values for each trajectory
RHV(10)	$\rho$ -values for equipotential lines
SPCH	space charge indicator switch
ST, ST2	$\sin \theta, \sin^2 \theta$
T0, T1, T2, . . .	temporary storages
TA(25)	$\theta$ -mesh values
TAU02	$\tau_0^2$
TH	variable of integration, $\theta$
TH0	initial cone angle, deg
TH1	initial cone angle, deg
TH2	collector angle at which surface charge is zero, deg
THD(10)	$\dot{\theta}$ array
THF	$\theta_f$
THMD(25)	$\theta$ -mesh values, deg
THSDEL	$\theta$ step-size increment, deg
THSW	$\theta$ switch for step-size control
THTD(10)	$\theta$ -coordinate of trajectory, deg
THD2	$\dot{\theta}^2$
THTR	$\theta$ -coordinate of trajectory, rad
THRZ	$\theta$ in r-z coordinate system
V(17, 25)	potential inside spherical collector
V0	initial normalized electrical potential, $V_0$
VR	interpolated potential in r-z system
VSMI(10)	$v_i$ array; beam velocities
VT(10)	array of initial voltages
W(16)	Runge-Kutta storage area in r-z system

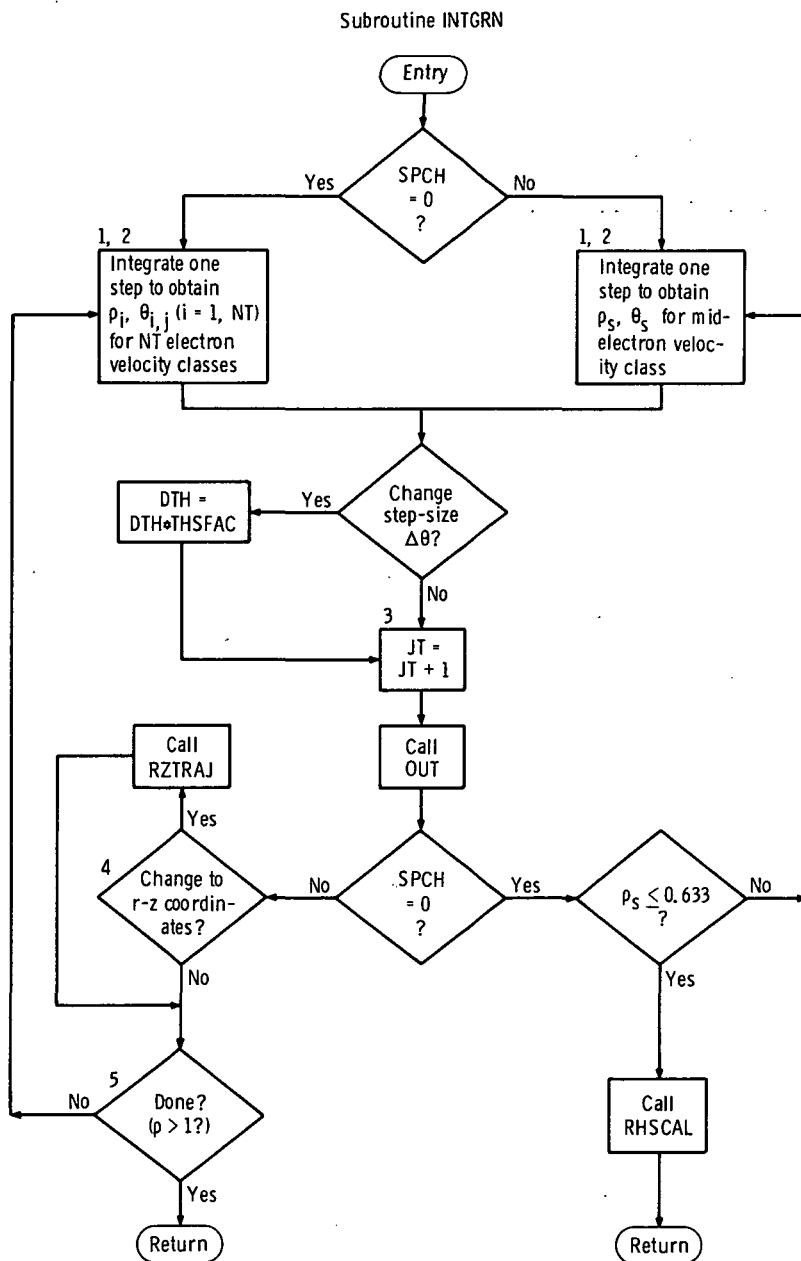
XCTR	value of source term at center of sphere
XT(25, 16)	source term needed for solution to Poisson's equation
Y(16)	Runge-Kutta storage area in $\rho$ - $\theta$ system
Z, ZP	$z, z'(\partial z/\partial r)$
Z1P	$\left. \begin{array}{l} z'_1 \\ z_2, z'_2 \end{array} \right\}$ miscellaneous storages for independent variables in cylindrical coordinate system
Z2, Z2P	
ZJ0	initial current density, $J_0, A/cm^2$
ZI0	initial current, $I_0, A$
ZKP	perveance, $K_p, A/V^{3/2}$
ZED	rectilinear coordinate, $z$



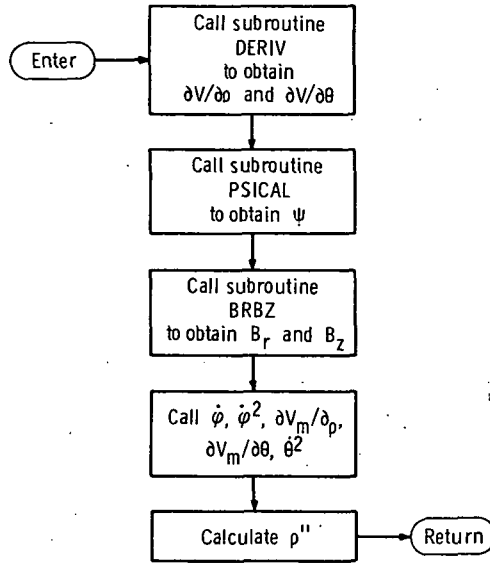
## APPENDIX D

### FLOW CHARTS

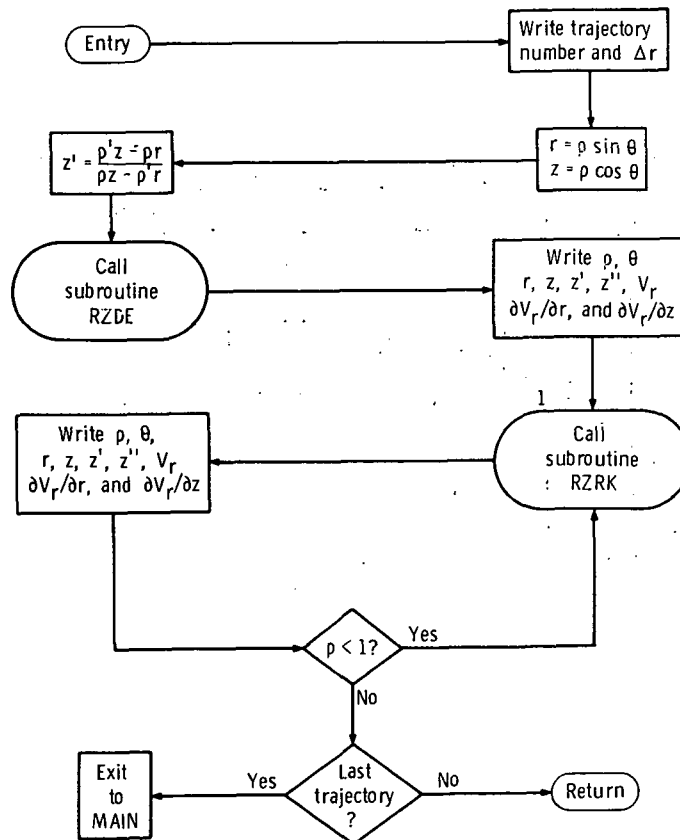
Flow charts are presented only for those five subroutines, INTGRN, DE, RZTRAJ, VFIELD, RHSCAL, which might not otherwise be easily understood. Diamond-shaped blocks indicate decision-making points in the subroutines. Numbers appearing on blocks refer to the corresponding FORTRAN statement numbers in the subroutines.



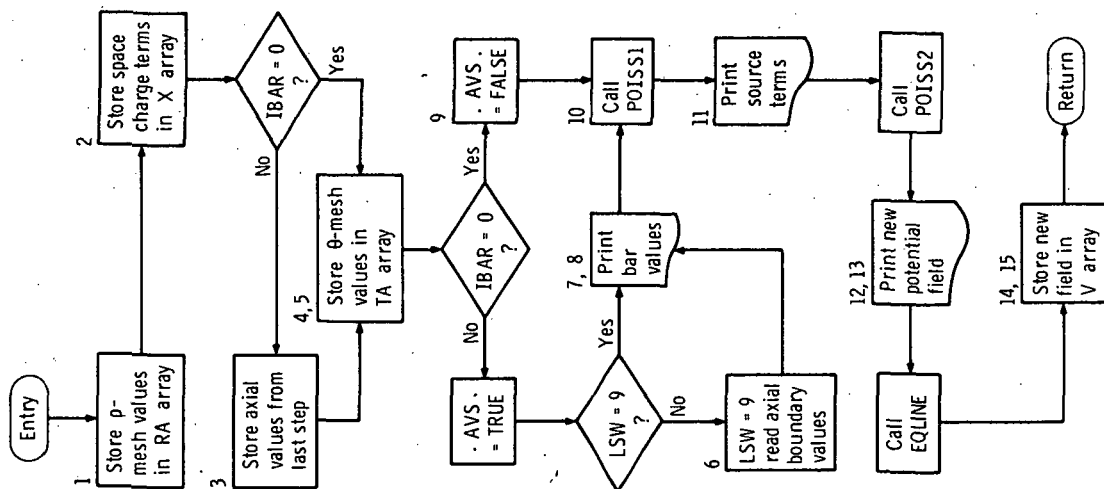
# Subroutine DE



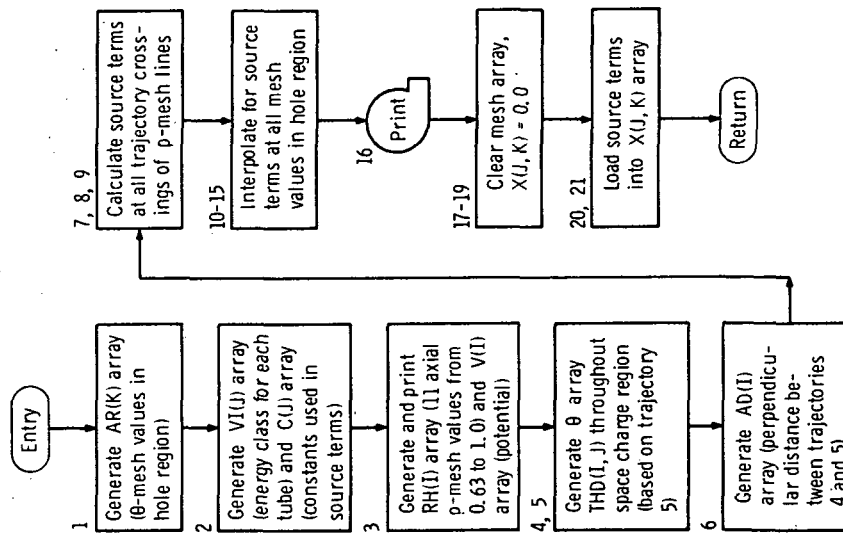
# Subroutine RZTRAJ



Subroutine VFIELD



Subroutine RHSCAL



## APPENDIX E

### MAGNETIC FIELD CALCULATIONS

$$B_z^0(0, z) = \frac{B_0}{\pi} \left[ \pi - \tan^{-1} \left( \frac{a}{-z} \right) - \frac{x}{1+x^2} \right] \quad (E1)$$

where  $x = z/a$ . Then,

$$\begin{aligned} B_z^I(0, z) &= -\frac{2B_0}{\pi a} \times \frac{1}{(1+x^2)^2} \\ B_z^{II}(0, z) &= \frac{8B_0 x}{\pi a^2} \times \frac{1}{(1+x^2)^3} \\ B_z^{III}(0, z) &= \frac{8B_0}{\pi a^3} \times \frac{1-5x^2}{(1+x^2)^4} \\ B_z^{IV}(0, z) &= -\frac{48B_0 x}{\pi a^4} \times \frac{3-5x^2}{(1+x^2)^5} \\ B_z^V(0, z) &= -\frac{48B_0}{\pi a^5} \times \frac{3-42x^2+35x^4}{(1+x^2)^6} \\ B_z^{VI}(0, z) &= \frac{4 \times 480B_0 x}{\pi a^6 (1+x^2)^7} (3-14x^2+7x^4) \\ B_z^{VII}(0, z) &= \frac{12 \times 480B_0}{\pi a^7 (1+x^2)^8} (1-27x^2+63x^4-21x^6) \\ B_z^{VIII}(0, z) &= -\frac{12 \times 14 \times 480B_0 x}{\pi a^8 (1+x^2)^9} (5-45x^2+63x^4-15x^6) \\ B_z^{IX}(0, z) &= -\frac{12 \times 14 \times 480B_0}{\pi a^9 (1+x^2)^{10}} (5-220x^2+990x^4-924x^6+165x^8) \\ B_z^X(0, z) &= \frac{14 \times 48 \times 480B_0 x}{\pi a^{10} (1+x^2)^{11}} (135-1980x^2+5346x^4-3564x^6+495x^8) \\ B_z^{XI}(0, z) &= \frac{14 \times 45 \times 48 \times 480B_0}{\pi a^{11} (1+x^2)^{12}} (3-195x^2+1430x^4-2574x^6+1287x^8-143x^{10}) \\ B_z^{XII}(0, z) &= -\frac{28 \times 45 \times 48 \times 480B_0 x}{\pi a^{12} (1+x^2)^{13}} (231-5005x^2+22022x^4-28314x^6+11011x^8-1001x^{10}) \end{aligned} \quad (E2)$$

To simplify these expressions, let

$$\begin{aligned}
 T_3 &= 1 - 5x^2 \\
 T_4 &= 3 - 5x^2 \\
 T_5 &= 3 - 42x^2 + 35x^4 = 3 - 7x^2(6 - 5x^2) \\
 T_6 &= 3 - 14x^2 + 7x^4 = 3 - 7x^2(2 - x^2) \\
 T_7 &= 1 - 27x^2 + 63x^4 - 21x^6 = 1 - 3x^2[9 - 7x^2(3 - x^2)] \\
 T_8 &= 5 - 45x^2 + 63x^4 - 15x^6 = 5 - 3x^2[15 - x^2(21 - 5x^2)] \\
 T_9 &= 5 - 220x^2 + 990x^4 - 924x^6 + 165x^8 = 5 - 11x^2\left\{20 - 3x^2\left[30 - x^2(28 - 5x^2)\right]\right\} \\
 T_{10} &= 135 - 1980x^2 + 5346x^4 - 3564x^6 + 495x^8 \\
 &= 9\left(15 - 11x^2\left\{20 - x^2\left[54 - x^2(36 - 5x^2)\right]\right\}\right) \\
 T_{11} &= 3 - 195x^2 + 1430x^4 - 2574x^6 + 1287x^8 - 143x^{10} \\
 &= 3 - 13x^2\left(15 - 11x^2\left\{10 - x^2\left[18 - x^2(9 - x^2)\right]\right\}\right) \\
 T_{12} &= 231 - 5005x^2 + 22022x^4 - 28314x^6 + 11011x^8 - 1001x^{10} \\
 &= 11\left[21 - 13x^2\left(35 - x^2\left\{154 - x^2\left[198 - 7x^2(11 - x^2)\right]\right\}\right)\right]
 \end{aligned} \tag{E3}$$

Then, substituting these expressions for those in (E2), we now have

$$\begin{aligned}
B_Z^I(0, z) &= - \frac{2B_0}{\pi a (1+x^2)^2} \\
B_Z^{II}(0, z) &= \frac{8B_0 x}{\pi a^2 (1+x^2)^3} \\
B_Z^{III}(0, z) &= \frac{8B_0 T_3}{\pi a^3 (1+x^2)^4} \\
B_Z^{IV}(0, z) &= - \frac{48B_0 x T_4}{\pi a^4 (1+x^2)^5} \\
B_Z^V(0, z) &= - \frac{48B_0 T_5}{\pi a^5 (1+x^2)^6} \\
B_Z^{VI}(0, z) &= \frac{4 \times 480B_0 x T_6}{\pi a^6 (1+x^2)^7} \\
B_Z^{VII}(0, z) &= \frac{12 \times 480B_0 T_7}{\pi a^7 (1+x^2)^8} \\
B_Z^{VIII}(0, z) &= - \frac{12 \times 14 \times 480B_0 x T_8}{\pi a^8 (1+x^2)^9} \\
B_Z^{IX}(0, z) &= - \frac{12 \times 14 \times 480B_0 T_9}{\pi a^9 (1+x^2)^{10}} \\
B_Z^X(0, z) &= \frac{14 \times 48 \times 480B_0 x T_{10}}{\pi a^{10} (1+x^2)^{11}} \\
B_Z^{XI}(0, z) &= \frac{14 \times 45 \times 48 \times 480B_0 T_{11}}{\pi a^{11} (1+x^2)^{12}} \\
B_Z^{XII}(0, z) &= - \frac{28 \times 45 \times 48 \times 480B_0 x T_{12}}{\pi a^{12} (1+x^2)^{13}}
\end{aligned} \tag{E4}$$

Since

$$B_r(r, z) = -B^I(0, z) \frac{r}{2} + \frac{1}{1!2!} B^{III}(0, z) \left(\frac{r}{2}\right)^3 - \frac{1}{2!3!} B^V(0, z) \left(\frac{r}{2}\right)^5 + \frac{1}{3!4!} B^{VII}(0, z) \left(\frac{r}{2}\right)^7 - \dots \quad (E5)$$

We make the substitution  $r_2 = r/2$ , and nest as follows,

$$B_r(r, z) = -r_2 \left[ B^I - \frac{r_2^2}{1 \times 2} \left( B^{III} - \frac{r_2^2}{2 \times 3} \left\{ B^V - \frac{r_2^2}{3 \times 4} \left[ B^{VII} - \frac{r_2^2}{4 \times 5} \left( B^{IX} - \frac{B^{XI} r_2^2}{5 \times 6} - \dots \right) \right] \right\} \right) \right] \quad (E6)$$

and similarly,

$$B_z(r, z) = B^0 - r_2^2 \left[ B^{II} - \frac{r_2^2}{2^2} \left( B^{IV} - \frac{r_2^2}{3^2} \left\{ B^{VI} - \frac{r_2^2}{4^2} \left[ B^{VIII} - \frac{r_2^2}{5^2} \left( B^{X} - \frac{r_2^2}{6^2} B^{XII} - \dots \right) \right] \right\} \right) \right] \quad (E7)$$

## APPENDIX F

### DERIVATION OF EQUATIONS OF MOTION

The equations of motion as derived in reference 1, equations (B17) and (B18), are

$$\rho'\ddot{\theta} = \rho\dot{\theta}^2 + \rho \sin^2 \theta \dot{\phi}^2 - \rho''\dot{\theta}^2 + \frac{\eta}{R^2} \frac{\partial V}{\partial \rho} - \frac{\eta}{R} \sin \theta \dot{\phi} A_{\phi} - \frac{\eta}{R} \rho \sin \theta \dot{\phi} \frac{\partial A_{\phi}}{\partial \rho} \quad (F1)$$

$$\ddot{\theta} = -\frac{2\rho'\dot{\theta}^2}{\rho} + \sin \theta \cos \theta \dot{\phi}^2 + \frac{\eta}{\rho^2 R^2} \frac{\partial V}{\partial \theta} - \frac{\eta}{\rho R} \cos \theta \dot{\phi} A_{\phi} - \frac{\eta}{\rho R} \sin \theta \dot{\phi} \frac{\partial A_{\phi}}{\partial \theta} \quad (F2)$$

Solving these two equations simultaneously for  $\rho''$  yields

$$\rho'' = \rho + \frac{\rho \sin^2 \theta \dot{\phi}^2}{\dot{\theta}^2} + \frac{\eta}{R\dot{\theta}^2} f_1 + \frac{2\rho'\dot{\theta}^2}{\rho} - \frac{\rho' \sin \theta \cos \theta \dot{\phi}^2}{\dot{\theta}^2} - \frac{\rho'\eta}{\rho^2 R^2 \dot{\theta}^2} f_2 \quad (F3)$$

where

$$\left. \begin{aligned} f_1 &= \frac{1}{R} \frac{\partial V}{\partial \rho} - \sin \theta A_{\phi} \dot{\phi} - \rho \sin \theta \dot{\phi} \frac{\partial A_{\phi}}{\partial \rho} \\ f_2 &= \frac{\partial V}{\partial \theta} - \rho R \cos \theta A_{\phi} \dot{\phi} - \rho R \sin \theta \dot{\phi} \frac{\partial A_{\phi}}{\partial \theta} \end{aligned} \right\} \quad (F4a)$$

or, using the relations described in appendix D of reference 1, these expressions may be rewritten

$$\left. \begin{aligned} f_1 &= \frac{1}{R} \frac{\partial V}{\partial \rho} - \sin \theta \dot{\phi} \frac{\partial V_m}{\partial \theta} \\ f_2 &= \frac{\partial V}{\partial \theta} + \rho^2 R \sin \theta \dot{\phi} \frac{\partial V_m}{\partial \rho} \end{aligned} \right\} \quad (F4b)$$

Away from the entry hole, the magnetic field terms  $\dot{\phi}$ ,  $A_{\phi}$ , and  $V_m$  are negligible. Therefore, in this region equation (F3) may be expressed



$$\rho'' = \rho + \frac{\eta}{R^2 \dot{\theta}^2} \times \frac{\partial V}{\partial \rho} + \frac{2\rho'^2}{\rho} - \frac{\rho' \eta}{\dot{\rho}^2 R^2 \dot{\theta}^2} \times \frac{\partial V}{\partial \theta} \quad (\text{F5})$$

using equation (B16) of reference 1 as

$$\dot{\theta}^2 = \frac{2\eta V_0(\epsilon_i + V)}{R^2 \rho^2 \left[ 1 + \left( \frac{\rho'}{\rho} \right)^2 \right]} \quad (\text{F6})$$

and, with the appropriate substitutions, we may express this equation in cylindrical coordinates

$$z'' = \frac{\frac{\partial V}{\partial z} - z' \frac{\partial V}{\partial r}}{2 \left[ \frac{\epsilon_i + V}{1 + (z')^2} \right]}$$

## APPENDIX G

### MATHEMATICAL SYMBOLS

$A$	area of annulus, $\text{cm}^2$
$a$	radius of collector entry hole, cm
$B_r$	r-component of potential field, $\partial V_m / \partial r$ , G/cm
$B_z$	z-component of potential field, $\partial V_m / \partial z$ , G/cm
$B_0$	magnetic flux density, G
$b$	radius of electron beam at injection, cm
$E$	$v_i + V$
$I$	current, A
$J$	current density, $\text{A}/\text{cm}^2$
$K_p$	perveance, $\text{A}/\text{V}^{3/2}$
$R$	unreduced radius of spherical collector, cm
$r, z$	cylindrical coordinates
$u$	electron energy
$V$	normalized electric potential
$V_m$	magnetic field potential
$V_r$	$\partial V / \partial r$
$V_z$	$\partial V / \partial z$
$V_\rho$	$\partial V / \partial \rho$
$V_\theta$	$\partial V / \partial \theta$
$v_i$	$i^{\text{th}}$ normalized injection energy class
$\epsilon_0$	permittivity of free space, $8.86 \times 10^{-14} \text{ F}/\text{cm}$
$\eta_e$	electron charge-mass ratio, $\text{charge}/\text{kg} \times 10^{11}$
$\rho$	normalized radius vector
$\bar{\rho}$	unnormalized radius vector, cm
$\rho_e$	space charge density, $\text{C}/\text{cm}^3$
$\tau_0$	$R / (2\eta V_0)^{1/2}$
$\theta, \varphi$	polar and azimuthal spherical coordinate angles

## REFERENCES

1. Kosmahl, Henry G.: A Novel, Axisymmetric, Electrostatic Collector for Linear Beam Microwave Tubes. NASA TN D-6093, 1971.
2. Reese, Oliver W.: Numerical Method and FORTRAN Program for Solving Poisson's Equation Over Axisymmetric Regions of a Sphere. NASA TN D-6438, 1971.



POSTMASTER: If Undeliverable (Section 158  
Postal Manual) Do Not Return

---

*"The aeronautical and space activities of the United States shall be conducted so as to contribute . . . to the expansion of human knowledge of phenomena in the atmosphere and space. The Administration shall provide for the widest practicable and appropriate dissemination of information concerning its activities and the results thereof."*

— NATIONAL AERONAUTICS AND SPACE ACT OF 1958

## NASA SCIENTIFIC AND TECHNICAL PUBLICATIONS

**TECHNICAL REPORTS:** Scientific and technical information considered important, complete, and a lasting contribution to existing knowledge.

**TECHNICAL NOTES:** Information less broad in scope but nevertheless of importance as a contribution to existing knowledge.

**TECHNICAL MEMORANDUMS:** Information receiving limited distribution because of preliminary data, security classification, or other reasons.

**CONTRACTOR REPORTS:** Scientific and technical information generated under a NASA contract or grant and considered an important contribution to existing knowledge.

**TECHNICAL TRANSLATIONS:** Information published in a foreign language considered to merit NASA distribution in English.

**SPECIAL PUBLICATIONS:** Information derived from or of value to NASA activities. Publications include conference proceedings, monographs, data compilations, handbooks, sourcebooks, and special bibliographies.

**TECHNOLOGY UTILIZATION PUBLICATIONS:** Information on technology used by NASA that may be of particular interest in commercial and other non-aerospace applications. Publications include Tech Briefs, Technology Utilization Reports and Technology Surveys.

*Details on the availability of these publications may be obtained from:*

**SCIENTIFIC AND TECHNICAL INFORMATION OFFICE  
NATIONAL AERONAUTICS AND SPACE ADMINISTRATION  
Washington, D.C. 20546**